HHS Public Access

Author manuscript

Adv Healthc Mater. Author manuscript; available in PMC 2023 May 01.

Published in final edited form as:

Adv Healthc Mater. 2022 May ; 11(9): e2102087. doi:10.1002/adhm.202102087.

Medical applications of porous biomaterials: features of porosity and tissue-specific implications for biocompatibility

Jamie L. Hernandez, **Kim A. Woodrow**

3720 15th Ave NE, Seattle, WA 98195, USA

Abstract

Porosity is an important material feature commonly employed in implants and tissue scaffolds. The presence of material voids permits the infiltration of cells, mechanical compliance, and outward diffusion of pharmaceutical agents. Various studies have confirmed that porosity indeed promotes favorable tissue responses, including minimal fibrous encapsulation during the foreign body reaction (FBR). However, increased biofilm formation and calcification is also described to arise due to biomaterial porosity. Additionally, the relevance of host responses like the FBR, infection, calcification, and thrombosis are dependent on tissue location and specific tissue microenvironment. In this review, we discuss the features of porous materials, and the implications of porosity in the context of medical devices. Common methods to create porous materials are also discussed, as well as the parameters which have been used to tune pore features. Responses towards porous biomaterials are also reviewed, including the various stages of the FBR, hemocompatibility, biofilm formation, and calcification. Finally, these host responses are considered in tissue specific locations including the subcutis, bone, cardiovascular system, brain, eye, and female reproductive tract. We highlight the effects of porosity across the various tissues of the body and emphasize the need to consider the tissue context when engineering biomaterials.

Graphical Abstract

woodrow@uw.edu .

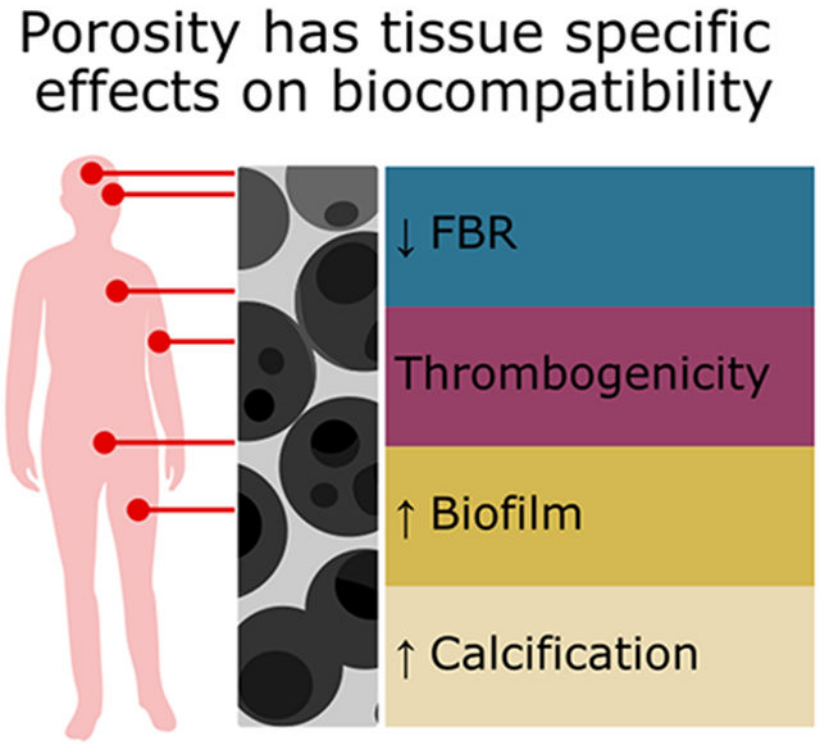

Porosity is an important biomaterial feature which enables biomaterial functionality and the capacity for cell integration, which is commonly characterized as a response with greater biocompatibility. In this review, we discuss methods used for fabricating porous materials, the effect porosity and specific pore size has on various host responses, and the responses which occur in tissue-specific microenvironments.

Keywords

biomaterials; porosity; foreign body reaction; biofilm; hemocompatibility

1. Introduction

Biomaterial selection dictates the functionality of medical devices – such as drug delivery systems, grafts, sensors, electrodes, and protheses. One of the most important determining factors of device success is implant safety and biocompatibility, which can be regulated by biomaterial composition and architecture.[1] Tissue mimicry can inform functional and biocompatible material designs.[2] One of the most notable features of tissue matrices is porosity, which is defined as having an architecture with interconnecting open spaces.[3] Pores allow for a multitude of material functions that include: cell integration with and into the material;[3,4] inward dispersion of oxygen, nutrients, analytes, and outward diffusion of pharmaceutical agents;[5,6] angiogenesis;[5,7,8] and pro-healing responses from immune cells[9–11] that can affect the foreign body reaction (FBR).[6,12–14] The FBR describes the innate response towards foreign materials, which results in immune cell infiltration at the material surface and the development of a fibrous capsule, or avascular scar tissue growth

which encapsulates the implant.[1,12,13] Such a response must be controlled, as a fibrous capsule can cause the patient pain, deform materials, alter the functional mechanics of the implant, limit drug release, and impede signals from electrodes and sensors.[1] Therefore, biocompatibility and the FBR not only have implications for patient wellbeing, but also material functionality.

Indeed porosity, and specific pore sizes, have shown to be a determining factor of biocompatibility with reduced fibrous capsule formation and increased angiogenesis when subcutaneously implanted.[10,15,16] Depending on the intended function of the implant and the local tissue microenvironment, biological responses other than tissue integration or the FBR may be more significant in determining implant acceptability. Further, the host response has been observed to vary between different tissue microenvironments.[17–19] Therefore greater consideration of tissue specific responses towards material porosity and specific pore size is needed to better inform truly biocompatible outcomes.

Although the FBR is the main consideration for material biocompatibility, the resulting FBR can be beneficial in some cases. For devices requiring osseointegration, calcification and an encapsulating FBR can be beneficial for generating integrated and mechanically stable tissue.[1,20,21] Generalizing the FBR has also caused clinical issues, especially for porous devices in the female reproductive tract, where dampened tissue-integrative responses commonly lead to rejection of implants like surgical mesh.[22] Porous material can also be at an increased risk of biofilm formation – an infection of bacterial communities on the material surface – especially where tissue integration is low, and microflora tolerance is promoted.[23] Although the FBR, calcification, and biofilms are all important concerns for cardiovascular implants, hemocompatibility must be considered for any material that is designed to be blood-contacting. Blood is protein rich and composed of leukocytes and platelets which can initiate inflammation or thrombosis in response to biomaterial surfaces, potentially resulting in fatal thromboembolization.[24–26] Local tissue microenvironment and implant function are therefore crucial considerations when engineering material features such as porosity.

In this review, we discuss the medical applications for porous materials and various methods for fabricating porous materials for research. We further summarize the biological responses to biomaterial implants including the FBR, hemocompatibility, biofilm formation, and calcification, as well as the specific effect porosity has on these pathologies. Tissue-specific responses to porous biomaterials are additionally discussed, highlighting the beneficial and negative applications of porosity in foreign bodies. Here, we emphasize the need for greater synchrony between the knowledge of biomaterial engineering and local tissue physiology. Information presented in this review should also motivate the need to characterize materials in relevant tissue compartments, as well as the existing need for developing improved tissue models. Further research of the biological mechanisms behind specific host responses could also inform the development of such models, as well as the design of materials which can exploit these responses. Considering the dedication of this special issue, we highlight the pioneering and ongoing work by members of Professor Buddy Ratner’s Biomaterials Group.

2. Definitions, methods, and implications of material porosity

2.1. Definitions and measurements of porous materials

Porosity is defined as the void of material, and is further characterized by the interconnections, or throats, between these pores, and walls or struts of the medium which forms the 3D structure (Figure 1).[3] Features of pores, throats, or struts are characterized by their size, shape, organization, density, and homogeneity. Traditionally, pore scale is delineated as macroporous when greater than 50 nm, mesoporous between 2 nm and 50 nm, and microporous when smaller than 2 nm.[27–29] Nanoporosity is also used to describe materials within the nano-scale range, with pore diameters between 1 and 100 nm.[28] Spherical, tubular, and random pore structures are commonly observed in porous materials, but novel fabrication methods are continuing to develop complex, high-resolution geometries,[30–33] and even materials with transforming topologies.[34] The geometry of these pores and interconnections are further defined as either closed, open, or blind-ended.[3]

Materials with porous features are mainly characterized by pore size or by the percent or ratio of porosity in the medium. For fibrous porous materials, strut or fiber diameter is also an important feature to characterize. Pore and strut size is most commonly estimated using imaging.[3] Methods such as optical microscopy, scanning electron microscopy (SEM), and transmission electron microscopy (TEM) can capture sections or regions of the material, then image analysis software can measure the pore or strut size features within the region of interest.[3] While these methods are simple, intuitive for assessing the material morphology, and avoid preparation methods that may modify native microstructures, imaging methods fail to capture the complete 3D structure of the material.[3] Other methods such as mercury and flow porosimetry can also quantify pore size as measured by the differential gas pressure of mercury or the measured pressure of a wetting fluid (P). However, these methods cannot measure closed pores and may have variable accuracy depending on surface and wetting fluid interactions.[3,27] Using the Washburn equation (Equation 1) or similarly the Young-Laplace formula, pore diameter (D) is calculated as a function of the surface tension of mercury or the wetting liquid (γ), and the contact angle of mercury or the wetting liquid and the sample (θ).[3]

$$D = \frac{-4\gamma\cos(\vartheta)}{P} \quad (1)$$

Measurements of porosity, or void fraction, are reported as either a percent or ratio (ε) of the pore volume (V_P) to the total bulk volume of the material (V_T). Materials are considered to have low porosity when $\varepsilon < 30\%$.[35] Pore volume is typically calculated using the density of the material used (ρ_m) and the mass of the sample (m_S).[3,27] Another simple way to calculate porosity uses Archimedes principle, which states that the volume of a fully emersed body is equal to the volume of water displaced. Pore volume can be calculated by the difference of wet and dry material weight, while total volume can be calculated by the difference of wet and fully submerged material. However, this method is not accurate for hydrophobic materials due to poor water penetration.[3] Equation 2 shows these calculations of percent porosity.

$$\%\ Porosity = 100 \times \varepsilon = 100 \times \frac{V_p}{V_T} = 100 \times \left(V_T - \frac{m_s}{\rho_m}\right) \Big/ V_T \quad (2)$$

2.2. Methods for fabricating porous materials

Materials with macroscale pores can be fabricated using a variety of techniques. These methods can be generalized as either subtractive or additive: either creating pores through the removal of sacrificial materials called porogens, or manufacturing walls/struts to surround open spaces, respectively.[27,30,36,37] Porosity can be an inherent feature of crystalline structures, but the resulting pores typically have molecular dimensions.[27] Here, we will focus on some of the most utilized methods that create tissue-scale, macro porous biomaterials. A summary of porous fabrication methods and resulting pore characteristics is listed in Table 1 and can be seen in Figure 2.

2.2.1 Subtractive methods—Perhaps the most frequently employed progeny leaching method for researching the effect of porosity on biocompatibility is sphere tinplating (Figure 2A).[4,9,10,38–43] Devices including hemodialysis grafts[44] and supraciliary drainage implants for glaucoma treatment[45,46] are fabricated using sphere templating, illustrating the translatability of this method. Sphere templating is a subtractive method which creates pores by first forming an array of sintered sphere microparticles, then filling the spaces of the array with polymer precursors, solidifying the polymer, and finally removing the beads so that just the polymer scaffold remains.[47] Pore size and porosity is therefore controlled by the geometry of the beads, which are commonly composed of polymers like poly(methyl methacrylate) (PMMA).[7,9,10,40,48–50] Similarly, salt particles are commonly used as a porogen in solvent cast and hydrogel materials (Figure 2B).[5,51–53] Although a wide range of pore sizes have been achieved,[5,51–53] salt crystals yield irregular pore geometries.[40] Various porous materials have been created with sphere templating, commonly UV polymerizable polymers like poly(hydroxyethyl methyacrylate) (poly(HEMA)), as well as silica, carbon, and even metals.[4,9,10,38,39,41–43,47,54] Selective UV polymerization can also be used as a strategy for patterning voids into materials using photolithography, which creates channels in materials using a 2D mask pattern with macro- or nanoscale pore diameter precision, and can be combined to create complex structures in combination with other fabrication methods.[54,55]

Freeze-drying or freeze casting is another subtractive method used commonly for making porous materials (Figure 2C). The freeze-casting process starts from a crosslinked or colloidal suspension commonly composed of an aqueous polymer solution. This solution is added to a mold, frozen, then sublimated to remove regions of solidified ice crystals.[56,57] Various parameters in the freezing process can modify pore size and various polymers can be utilized. However, pore size can be difficult to tune with freeze-drying, the processing time can be long, energy intensive, and the resulting materials often have poor mechanical integrity.[5,36,56,58] Alterations on the freeze-drying process include directional freezing to control pore morphology,[5,56,59] freeze-extraction and freeze-gelation to eliminate the time

and energy needed for the freeze-drying process,[60] as well as added freeze-thaw cycles to increase scaffold toughness.[5,61]

Comparably, gas foaming methods use supercritical carbon dioxide as a porogen in polymer solutions, which expands to create pores when returned to a gas state (Figure 2D).[5,62] One of the main benefits of this technique is that organic solvents are not used, which can have adverse biological and environmental effects.[62–65] Due to low solubility of CO_2 in hydrophobic polymers, the use of surfactants and water emulsions are commonly used, although these factors alter pore size.[62,63] The resulting high porosity from both gas foaming and freeze casting make both of these methods widely used for tissue engineered scaffolds in general, and can generate materials with pores sufficiently large for bone ingrowth.[36,66,67]

Decellularizing tissues is another strategy commonly investigated to create biocompatible and porous materials, used for notable tissue scaffold applications like bioartificial hearts.[68] However, the resulting scaffolds often lack mechanical integrity, or contain pores only a few nanometers in diameter which are too small for host cells to repopulate.[69–72] To mitigate this, decellularized tissues have been additionally processed with subtractive methods to increase porosity, but this further sacrifices mechanics.[72] Additive methods combined with these scaffolds can reinforce tissues, but at the disadvantage of decreased porosity.[70] Emerging research is therefore more focused on utilizing extracellular matrix (ECM) components from decellularized tissues as a medium with additive methods like electrospinning, 3D printing, or molding for both porous and robust materials.[71–74]

2.2.2 Additive methods—Recent advances in 3D printing technology have made this an increasingly popular method for creating porous scaffolds (Figure 2E).[31] 3D printing broadly includes additive manufacturing techniques capable of precision patterning materials.[30] Thus, pores can be formed through the spacing of deposited or cured materials. For a comprehensive description of these 3D printing methods, the reader is directed to the review by Ngo, et al..[30] Various materials are amenable for 3D printing techniques, including polymers, ceramics, metals, and even living cells.[30,31] The ease of making larger pore features with this method makes printing bone scaffolds relevant,[36,75] but bioprinting has made a variety of tissues and vasculature structures possible,[76] and 3D printing methods can be even amenable for drug delivery.[77] Some printing methods like stereolithography have a high feature resolution of less than 10 μm, and greater porosity can also be achieved by combining subtractive methods like salt leaching.[78]

Meshes are commonly used in biocompatibility studies of porous features as these materials are truly porous, thin, tunable, and are clinically relevant to tissue support and hernia repair surgeries.[79] Electrospinning yields sheets of materials with nano- or micro-scale fibrous architectures, and is therefore commonly used for drug delivery research, tissue engineering, and study of the host response (Figure 2F).[18,80,81] Specifically, some of these applications include wound dressings,[82–85] vascular grafts,[86–91] and intravaginal dosage forms for antiretroviral drugs.[92–99] Additionally, this method is amendable to virtually any natural or synthetic polymer and can efficiently encapsulate physicochemically diverse pharmaceutical agents or growth factors.[81,100,101] Conventional spinning methods start

from a solution composed of desired polymers, agents, and a volatile solvent, which is loaded into a positively charged syringe. This charged solution is then extruded across from a negatively charged collector, so that fine fiber protrusions form from the tip of the needle, and deposit onto the collector as a sheet of solid, solvent-free material.[81,101] Various factors including polymer concentrations, flow rate, voltage, solvent, and modified collection targets with perforations or rotation can be altered to change the dimensions and alignment of the electrospun fibers, and therefore pore size and porosity.[80,102–104] However, the resulting porosity from electrospun fibers is typically lower than other scaffold fabrication methods (Table 1). Much like 3D printing, the electrospinning process can be adapted with subtractive methods like porogen leaching and freeze casting to improve porosity.[32,105,106]

2.3. Implications of porosity on biomaterial properties

When considering material porosity, context is important for evaluating porosity effects on performance outcomes. For implants and tissue engineering scaffolds, voids are typically intended to permit cell migration, the influx of oxygen and nutrients to sustain these cultures, and the outflux of metabolic wastes.[5,120] For drug delivery, these voids are intended to be saturated with biological fluids, thereby enabling drug release by modes of outward drug diffusion or hydrolysis mediated material erosion.[29,121,122] Thus, permeability is an important effect of porosity and influenced by pore size and their interconnections, bulk material dimensions, surface characteristics of the material such as hydrophilicity, and pressure differences.[3,27] Capillary action is one mechanism of permeability, which mediates uptake of fluids within pores due to pore size and surface tension of the solution with the material walls.[123,124] While decreased pore or throat size may limit permeation of agents such as cells via size exclusion,[5,41] capillary action dictates an increased fluid permeation distance with smaller pore diameters.[124] Therefore, the impact of pore size on biological fluid permeation depends on the target permeating agent and the surface interactions of the fluid and material walls.

Porosity also impacts material surface-to-volume ratios – as greater percent porosity increases material surface area, and larger pores with constant percent porosity decreases material surface area.[122] Wall or strut size is therefore also a determinant of the surface-to-volume ratio. Materials with larger surface-to-volume ratios can enable greater access for cell attachment,[115,121] or increase drug release rates (described in section 2.3).[122] The presence of pores and walls also implies the presence of texture or roughness at the material surface, which additionally impacts cell attachment, protein absorption, inflammatory responses, platelet activation, and bacterial adhesion.[25,37,125–128] Increased porosity also decreases scaffold support which can inversely affect the mechanical integrity of the material.[36]

While attachment, drug release, material erosion, and mechanical properties are impacted relatively by porosity, the specific selection of the material will also have a critical impact on these attributes. Further, specific material or polymer composition will provide features like erodibility or swellability that can alter pore geometry *in situ* over time.[129,130] Specific pore shape, strut curvature, and alignment has also shown determining effects on cellular

responses.[33] To delineate the contribution of porosity alone, research commonly assesses chemically identical materials with multiple pore sizes (see Table 1 for methods to alter pore size per method),[10,15,80,131] or screens various materials and assesses the correlation of pore size effects in addition to the composition.[16,132–134] The effect by pores as opposed to wall structure has also been studied by compressing porous materials after identical fabrication methods.[80]

2.4. Effects of porosity on drug delivery systems

Drug delivery is one important application of biomaterials and is impacted in various ways by porosity. The release of drug into biological solution requires both drug dissolution and diffusion. Within a polymer matrix, drug release can occur by the erosion of the encapsulating polymer or by diffusion through a polymer matrix - both of which may be impacted by porosity.[135] The Higuchi Equation separately considers non-porous and porous drug release systems (Equation 3), is widely used, and simply estimates the flux of total drug release (Q) over time (t) per unit area (A) considering drug dissolution and diffusion.[135,136] Further, this equation is modeled one-dimensionally for a rate-limiting ointment film releasing drug into skin under sink conditions, where D is the diffusion coefficient of drug into the biological solution, ε is the porosity of the material, τ is the tortuosity – or the size and branching of the interconnected pores, C_0 is the initial concentration of drug, and C_S is the drug solubility within the matrix.[137]

$$Q = A\sqrt{\left(\frac{D\varepsilon}{\tau}\right)(2C_0 - C_S)C_S t} \tag{3}$$

This form of the Higuchi equation accounts for a change in the effective diffusion constant for porous mediums, which increases with higher porosity and lower tortuosity, thereby also increasing drug release.[136,138] The diffusion coefficient also changes dynamically in response to matrix swelling.[136] In the case of porous mediums, swelling alters pore size and tortuosity overtime.[138] The presence of porosity in a drug delivery system described by the Higuchi equation also modifies the drug solubility factor (C_S), which accounts for the partition of drug concentrated inside and outside of the pores.[135,136]

Factors of porosity such as the increased surface area, decreased path of diffusion within the matrix, and greater inward or outward flux may increase drug release rates, and specifically drug release mediated by polymer scaffold erosion.[29,122] Experimentally, materials with larger surface-to-volume ratios – like materials with high porosity – have shown faster, diffusion mediated release.[29,122] However, this correlation is material dependent, as polymers with acidic byproducts such as poly(lactic acid) (PLA) and poly(lactic-co-glycolic acid) (PLGA) show increased drug release for materials with lower porosity, lower permeability, and thicker material walls. Accumulation of carboxylic groups within pores accelerates the hydrolysis of these degradable polymers.[139–141] Higher porosity can also imply a decreased deliverable dose or a reduction of the polymer which controls agent release.[121] Therefore, the release kinetics of drug delivery systems are heavily influenced by both material composition, material pore morphology, and the interaction of these factors.

3. Biocompatibility in respect to porosity

A modern definition of biocompatibility put forth by Crawford et al., is “the ability of a material to locally trigger and guide the proteins and cells of the host toward a non-fibrotic, vascularized reconstruction and functional tissue integration.”[1] The effect of material porosity on biocompatibility has been extensively studied, repeatedly showing that porosity improves tissue healing responses and decreases scar tissue growth.[4,10,13,33,38,39,80,142–144] Considering our tissue-specific focus here, we have broadened our definition of biocompatibility to consider the other factors which are critical to the success of the medical device. Beyond the FBR, this includes hemocompatibility, biofilm formation, and calcification – all of which have nuanced impacts by porosity. Table 2 and Figure 3 includes a summary of porosity effects on the various aspects of biocompatibility discussed in this section.

3.1. Stages of the foreign body reaction in response to porosity and specific pore size

3.1.1. Greater surface-to-volume ratios can increase specific protein absorption—

The FBR can be characterized by five phases.[1,12,13] First, local tissue and blood proteins will adhere to the material surface within an order of seconds following implantation. In this first phase, a provisional matrix is formed around the implant, including clotting proteins like fibrinogen, fibronectin, and vitronectin, as well as opsonins such as proteins belonging to the classical complement system pathway and immunoglobulins (IgG).[12,13] This provisional matrix develops rapidly into a thrombus composed mainly of fibrin.[13] The composition of the provisional matrix changes dynamically over time following the Vroman Effect, as proteins absorb and desorb on the surface.[1,13,162] Bioactive agents in the provisional matrix – including cytokines, growth factors, and chemoattractants – can promote the activation, migration, proliferation, and polarization of immune cells and fibroblasts, thereby impacting the subsequent stages of the FBR.[162]

The magnitude of protein absorption is highly dependent on the type of material used, but is also increased by surface roughness.[13] Increased absorption is likely a factor of a greater surface area to volume ratio.[163] Greater porosity can therefore induce greater protein adhesion as well as the specificity of proteins that adhere to the surface. Jansson, et al., showed that titanium surfaces with pores between 0.2-0.3 μm absorbed two to eleven times more albumin and IgG than smooth titanium surfaces. While IgG may activate immune cells, albumin reduces platelet and neutrophil activation.[164] However, this effect is altered at the scale of protein-size, as was shown in a study by Richert, et al.. Nanoporous titanium surfaces with a mean pore diameter of 0.011 μm promoted fibrinogen, lysozyme, and human growth/differentiation factor-5 (GDF-5, osseogenic cell promoter) binding, and decreased absorbance of bovine serum albumin, IgG, fibronectin, and collagen as compared to non-porous surfaces.[165] The dimensions of IgG and fibronectin surpass this pore diameter, which likely explains this difference in absorption.[165]

Beyond pore size, the protein adhesion is also dependent on the geometry of the material walls or struts. Woo, et al. demonstrated that porous poly(L-lactic acid) (PLLA) scaffolds with nanofibrous walled pores (diameter = 0.05-0.5 μm) absorbed 4.2 times the protein compared with materials with solid walled pores (diameter = 250-420 μm). Additionally,

these nanofibrous materials specifically absorbed greater quantities of proteins implicated in cell attachment including albumin, fibronectin, vitronectin, and laminin.[166] Stochastic roughness, which may be created from materials with random pore morphology, has shown to increase absorbance of fibronectin, an ECM protein that promotes macrophage attachment.[162,163] Although informative to understand early mechanisms of the FBR, studies of protein adhesion alone are conducted *in vitro*. These studies therefore exclude competitive protein binding dynamics that will have determining effects on immune cell signaling and the final host response.

3.1.2. The effect of porosity on acute inflammation may not predict long-term responses—Following protein adhesion, the FBR enters the second phase known as acute inflammation.[1,13,162] Neutrophils are the first immune cells to infiltrate the material surface and act as the primary cell population during acute inflammation, along with mast cells, for a period of hours or less than a week.[13,162] Tissue damage from implantation, recognition of the provisionary matrix, recognition of the foreign body and/or bacterial infection may initiate neutrophil migration.[1,13] Studies have rarely focused on the biomaterial impact on acute inflammation, therefore not much is known about the effect of porosity or topography on this phase.[13] One study by van Tienen, et al. distinguished the one-week acute inflammatory response towards materials with porosities of 73% or 86% – both with pores 150-300 μm in diameter but varied by the throat diameter. A similar magnitude of neutrophil infiltration was observed towards both materials, despite differences in tissue ingrowth at later timepoints.[167] These studies focused on quantifying cell accumulation, but additional information on the cytokine release profile by neutrophils may better inform the factors that recruit, activate, and direct macrophage phenotypes.[13]

3.1.3. Chronic inflammation and macrophage polarization is controlled by pore size—Chronic inflammation defines the third phase of the FBR, and persists for two to three weeks with notable local responses from macrophages.[13] Macrophages have been characterized as the primary arbiter of the FBR, and are activated by cytokine signaling and by adhesion to the provisional matrix. Activated macrophages are described to exists in two main polarization states: the pro-inflammatory M1 phenotype and the anti-inflammatory M2 phenotype (illustrated in Figure 3A).[1,12,13] M1 macrophages kill pathogens, activate T-cells, degrade ECM proteins, are implicated in T helper 1 cell (Th1) responses to intracellular pathogens, and are associated with a FBR that has greater acute and chronic inflammation. M2 macrophages are further divided into M2a, M2b, M2c, and M2d phenotypes. All M2 subtypes are implicated in Th2 responses to extracellular pathogens, ECM synthesis, angiogenesis, and control over acute and chronic inflammation.[1,12,168] Although, M2b macrophages may also promote inflammation and M2d macrophages are implicated in wound healing as opposed to fibrosis.[168] Table 3 includes known inducers of these phenotypes, and factors which are secreted from these cell types.

These subtype delineations are known to be an oversimplification of macrophage behavior *in vivo*.[1,168] Additionally, absence or over-abundance of either pro-inflammatory and anti-inflammatory macrophages can lead to unfavorable FBR.[168] Beyond macrophages, cells of the adaptive immune system also play a role in the FBR.[9,169,170] Regulatory T-cells

(Tregs) have been implicated in pro-healing responses. Th1 cells increase inflammation and inhibit collagen deposition, while Th2 cells induce fibrosis and inhibit inflammation.[9,169] Further, T-cells may act on macrophages and influence their polarization through the release of cytokines, or by antigen presentation.[169]

The macrophage response to porous materials has been extensively studied. Sussman, et al. characterized macrophage phenotypes in response to sphere templated poly(hydroxyethyl methyacrylate) (pHEMA) materials with either 34 μm or 160 μm pores as well as non-porous pHEMA, as illustrated in Figure 3A. Inflammatory infiltrate was significant at the surface of non-porous implants but was minimal at the surface of either 34 or 160 μm porous materials. Within the fibrous capsule at the material interface, non-porous materials had M1 dominated responses, whereas porous materials had M2 dominated responses. Within the 34 μm pores, macrophages were more significantly M1 phenotypes, but were associated with greater vascularization and lower intrapore fibrosis. This distinction was not observed significantly in 160 μm-porous materials.[10] Sphere-templated pHEMA pores 100 μm in diameter have also been found to induce greater gene expression for inflammatory Th1 cells in comparison to 40 μm pores.[9]

Garg, et al. used electrospun polydioxanone materials with randomly conformed pore diameters averaging approximately 2, 22 and 30 μm, which increase with strut diameter. Macrophages seeded onto materials with larger pore and strut diameters resulted in greater M2 macrophage attachment (Figure 3A). Additionally, compressed materials with equivalent strut size, but reduced pore diameter, had reduced M2 attachment, indicating that the pore size is indeed the main contributor to macrophage polarization in these materials.[80] Using 3D printed polycaprolactone (PCL) box-shaped pores, Tylek, et al. illustrated that M2 differentiation is accompanied by macrophage elongation. Further, elongation is promoted with smaller, 40 μm pores (illustrated in Figure 3A).[33]

Bartneck, et al. also studied the effect of electrospun porosity on macrophage polarization, and inversely found 20 μm porous materials induced more M1 polarization and 100 μm materials induced greater M2 polarization as measured by 27E10+ and CD165+ surface markers, respectively. However, the cytokine profiles suggest the 20 μm materials initiate greater pro-angiogenic signaling, while greater pro-inflammatory expression is measured in response to 100 μm materials.[171] These results are still consistent with the consensus of work, as signaling cues have the largest downstream effect on the FBR, and illustrates the over simplification of the polarization model for macrophages. Moving to even larger pore size, Yin, et al. found increased M2 polarization and VEGF expression in response to materials with 360-μm pores as compared to 160-μm pores.[147] Combined with existing research, this suggests that a window of unfavorable immune responses may exist for pore sizes around 100 – 160 μm. In studies of meshes with pore diameters ranging between 460 μm and up to 4000 μm, more favorable responses have been seen with larger pores.[172,173] Pores larger than 1000 μm are said to prevent contact between filament associated inflammatory infiltrate, and therefore prevents the bridging of scar tissue.[173] However, the capability of having large scale pores is dependent on the three-dimensional thickness of the scaffold and the required mechanical properties. Overall, existing research suggests that despite difference in polymers, fabrication methods, and architecture, pore

sizes approximately 30-40 μm in diameter yield greater pro-healing immune cell responses at the material surface, and have been further associated with greater vascularization, a reduced fibrous capsule, and greater tissue integration.[4,7,9,10,14,38–40,80,146]

3.1.4. Foreign body giant cell formation is confounded by factors beyond porosity—The fourth phase of the FBR is foreign body giant cell (FBGC) formation. Multi-nucleated FBGCs form by the fusion of macrophages at the biomaterial surface.[1,13] This is a result of frustrated phagocytosis, where adherent macrophages attempt and fail to phagocytose the large implant, and is thought to be a mechanism to avoid apoptosis.[1,13,174] Cytokines IL-4 and IL-13 are implicated in FBGC formation and are considered to be derived from M2 macrophages, but distinctively express both pro-inflammatory and anti-inflammatory cytokines (Table 3).[13,168] Further, pro-healing growth factors, such as VEGF, are secreted by FBGCs,[175,176] as well as reactive oxygen species (ROS) and enzymes which contribute to material degradation and device failure.[13] The function of FBGCs in either a pro-healing or destructive FBR is not clearly defined, although these cell types likely contribute to both pathways depending on material features and time.[149,175,176]

In comparison to macrophage polarization, the relationship between pore size and FBGC formation is less consistent in the literature. Saino, et al. showed greater FBGC formation *in vitro* on PLLA non-porous films as opposed to electrospun nanofibrous and microfibrous materials.[148] Similarly, a study of highly porous (~85%) sphere templated polyurethane (PU) materials by Bezuidenhout, et al. found significantly reduced FBGC formation on materials with larger pore diameters (150-180 μm) when implanted subcutaneously in rats.[131] However, Lucke, et al. showed greater FBGC formation on porous electrospun PLA mesh surfaces than non-porous membranes, which were implanted intramuscularly in rats.[149] At early timepoints, the macrophage populations within and surrounding porous materials are consistent with the observations made by Sussman, et al. describing high M2 populations at the surface and high M1 populations within pores. However, after 56 days, the FBGC response was seen to be greater towards porous mesh materials, as compared to smooth, membrane implant controls.[10,149]

The discrepancy in the FBGC response towards porosity across these different studies could be confounded by additional factors which may influence the FBR. First, pore size is not reported for PLA meshes with high FBGC adhesion, and highly porous PU materials with low FBGC adhesion are not compared to a non-porous control.[131,149] Therefore, a window of high FBGC adhesion may exists for porous materials with small void diameters, as is observed for macrophage polarization. Second, FBGCs effect degradable PLA and bio-stable PU differently. While FBGCs can induce PU cracking, the scaffold is not degraded like PLA, which will change in structure as the material is eroded. Further, the resulting release of lactic acid from degraded PLA is known to promote inflammation.[131,149] However, reported FBGC responses from other *in vitro* studies of PLLA contradict what is observed *in vivo* for PLA electrospun materials, although differences in chirality and resulting changes in polymer crystallinity may confound this comparison.[148,149] Finally, the difference in implant site may also contribute to FBGC responses. Indeed, greater inflammatory responses have been observed towards materials implanted intramuscularly, as compared to materials implanted subcutaneously.[17] Thus, the effects of porosity on

FBGCs, and the effects of FBGCs on the FBR, are not simply positive or negative for wound healing. Future assessments to clarify the role of porosity on FBGCs and the resulting FBR should consider additional factors like material and local tissue environment.

3.1.5. Porous materials promote wound healing and limits fibrous capsule formation—In the final stage of the FBR, collagen rich scar tissue growth, known as fibrous capsule, commonly develops around biomaterials. In response to factors such as TGF-β released from cells like M2 macrophages, fibroblasts migrate to the surface of the biomaterial and generate ECM proteins like collagen which forms the fibrous capsule.[1,13] Macrophages may also secrete other factors such as matrix metalloproteinases (MMPs), which degrade ECM proteins as needed for tissue remodeling at the implant site.[13,168] Biomaterials become encapsulated by this largely acellular tissue, which can act as a barrier in applications like drug delivery, sensors, or electrodes, and additionally can alter local tissue mechanics and therefore tissue function.[1] Further, fibroblasts may differentiate into myofibroblasts, which can contract the tissue surrounding the biomaterial, potentially causing patient pain and device damage.[1,13]

In contrast to fibrous capsule formation, the desired outcome for most implanted biomedical materials is to functionally integrate into the surrounding tissue environment. Beneficial wound healing responses promote the regeneration of local tissue cell types, and the ingrowth of new vasculature, known as angiogenesis, to support the transport of oxygen and nutrients into developing tissue.[1,5,13,178] Angiogenesis is especially important in biomaterial scaffolds for tissue engineering, where cells must functionally inoculate the material structure. Without supporting capillaries, oxygen and nutrients can penetrate a distance of approximately 150-200 μm.[5]

A reduction in fibrous capsule size in response to porous materials was first observed by Karp, et al., where a difference in FBR was demarcated between commercial Millipore filters with pores 0.025-0.1 μm and 0.22-8.0 μm. In the materials with larger pores, a less developed fibrous capsule was observed with cells found inside the pores, more non-adherent macrophages between the implant and capsule, and many FBGCs.[15] Cells have been found to penetrate materials with pores as small as 0.8 μm, but an increase in pore size up to 9 μm further promoted vascularization.[16]

Studies of larger pore-size materials have indicated that the benefit of increased pore size on pro-healing and angiogenic responses has an upper limit. Sussman, et al. found that porosity overall reduced fibrosis. However, materials with 34 μm pores were permeated by cells with minimal collagenous growth and a greater density of blood vessels, while 160 μm pores contained a greater fraction of fibrotic tissue (Figure 3A).[10] Similar pHEMA scaffolds have found that implants and pore features remain intact out to 28 days.[4] In a study by Bezuidenhout, et al., materials with pore sizes ranging from 63 to 180 μm showed no statistical difference in vascularization.[131] Overall, porosity and pore sizes approximately 30-40 μm in diameter significantly impact the acceptability of local tissue responses when studied in rodent models (Figure 3A). Interestingly, this pore size is near twice the size of relevant cells – with rodent macrophages and fibroblasts measuring approximately 13 and

18 μm, respectively.[179,180] A summary of the effects from pore size on fibrous capsule formation and angiogenesis is illustrated in Figure 3A.

3.2. Hemocompatibility and thrombosis in response to material porosity

Medical devices that contact blood – such as dialyzers, drug delivery systems like nanoparticles, and cardiovascular devices including vascular grafts and stents – have unique considerations for biocompatibility.[181] Blood is composed of cells including erythrocytes, leukocytes, and platelets.[24] Materials that contact blood are therefore susceptible to inducing cell lysis, immune recognition (similarly described in sections 3.1.2 and 3.1.3), and especially thrombosis. No standards currently exist for assessing material hemocompatibility, nor is there a consensus on which materials are hemocompatible. Assessments of blood biocompatibility typically focus on thrombogenesis prevention,[152,182] but these assessments lack predictive value on biocompatibility. Excessive thrombosis can result in lethal thromboembolism or device occlusion, which can halt device function and downstream blood flow.[152] On the other hand, blood clotting on biomaterial surfaces can be beneficial to prevent hemorrhage and to act as a matrix for cell attachment.[152] In fact, adhered but non-activated platelets can be a natural passivating surface against thrombogenicity, so blood contacting materials like woven vascular grafts are commonly pre-clotted prior to implantation.[152,183] Thrombosis is also dependent on more than just surface interactions, but also specific blood chemistry and the mechanics of blood flow.[152,184]

In addition to the cellular components, blood is composed of important plasma proteins like albumin, fibrinogen, and immunoglobulins.[24] As described in the first phase of the FBR (section 3.1.1), blood serum proteins spontaneously absorb onto biomaterial surfaces after implantation due to the inherent blood contact which occurs with surgical procedures.[13] This phase is also the first step of the intrinsic clotting cascade involving a series of enzymatic response initiated by surface contact with a foreign material.[13,25] As stated in section 3.1.1, the larger surface area provided by greater material porosity can lead to greater protein adhesion on the material surface.[163] However, clotting responses are also protein specific, as albumin is generally considered passivating and fibrinogen is thrombogenic.[25] Protein conformation, and the change of protein composition on the surface dictated by the Vroman effect, also impacts hemocompatibility over time.[24,152] The second mechanism which coagulation can also occur by is the extrinsic pathway, which is activated by the release of tissue factor (TF) from injured vascular endothelial cells (ECs). ECs line blood vessels and are likely to be damaged with an incision or implant placement.[184] The activation of TF may also arise from inflammatory mechanisms from leukocytes at the material surface or by complement activation.[24,181,185]

Mechanical activation of platelets can also arise with both high and especially low fluid shear forces.[184] Indeed, simulated and experimental results have shown that 75 μm crevices in a surface can induce shear mediated thrombosis (Figure 3B).[151] Milleret, et al. found electrospun scaffolds with 5 μm material struts and an average pore diameter approximately 35 μm yielded greater platelet adhesion and activation than non-porous controls (Figure 3B). Materials with approximately 10 μm pores and struts less than

1 μm behaved comparably to non-porous materials (Figure 3B). Thrombosis was also independent of polymer used or hydrophilicity of the material, so the effect is attributed to the changes in topography.[133] Zhao, et al also found that materials with pores 2-5 μm induced statistically similar low platelet adhesion and high whole-blood compatibility as compared to smooth surfaces, while 35-45 μm porous materials yielded statistically greater platelet adhesion and lower whole blood compatibility (Figure 3B).[153] Overall, surface roughness associated with greater porosity can be considered more thrombogenic, but several studies support opposite findings.[186–188] Interestingly, these *in vitro* studies that find reduced platelet activation towards materials with greater porosity, and specifically materials with approximate 30 μm pore sizes, use static testing conditions and sodium citrate instead of heparin as an anti-coagulant to reduce fibrin formation.[187,188] Although the use of any anti-coagulant will alter thrombogenesis, sodium citrate is a calcium chelator, which is especially problematic for blood-biomaterial interactions because the removal of calcium will reduce platelet-surface interactions.[152] Responses may also be attributed to differences in strut geometry arising from different fabrication methods. The varied platelet response to porosity illustrates the complexity of blood-material interactions, as well as the need to standardize hemocompatibility assessment methods.

Interestingly, the materials which are the current standard for hemocompatibility – expanded polytetrafluoroethylene (ePTFE, Gore-Tex) and poly(ethylene terephthalate (PETE, Dacron) – have micron scale pores (~5 μm).[152,153,183] Porous materials permit tissue ingrowth and can affect mechanical compliance, both which can contribute to more favorable outcomes for hemocompatibility.[87,150] Clot formation is still observed on the surface of these materials, but this response is considered acceptable as long as the clot does not embolize.[152,183] The complex response of porous materials in the cardiovascular system are further discussed in Section 4.3.

The fluid dynamics of blood is another consideration for hemocompatibility. Porosity mediated water permeation is beneficial for transferring nutrients to cells within the tissue. However, greater permeation can increase platelet activation and lipid infiltration.[150] Additionally, materials with porosity higher than 50 mL of water min^{-1} cm^2 of material at a pressure of 120 mmHg can cause hemorrhage when treated with anti-coagulants.[132] Porosity and pore size importantly contribute to the complex interactions which occur between biomaterials and blood, and these generalized conclusions for thrombogenesis and platelet activation are summarized in Figure 3B. In general, smooth surfaces are typically preferred for improved hemocompatibility, but porous materials are often a necessary deign feature for blood contacting materials to permit suturing or for local tissue integration.[152] Section 4.3 includes a discussion of both hemocompatibility, endothelium passivation, and local tissue healing responses towards porous materials in the cardiovascular system.

3.3. Biofilm formation and the race for the surface on porous materials

Biomaterials can also initiate adverse responses by creating a new niche for foreign pathogens within the body. Indeed, the bacterial colonization of medical devices, known as biofilm formation, is one of the most frequent complications of clinical biomaterial use.[160,189] While the host immune system might normally clear invading bacteria, the

local fibrous capsule generated in response to the biomaterial creates an immune depressed environment, and bacterial colonies within a biofilm are protected by extracellular polymeric substances (EPS).[23,160] Thus, biomaterial surfaces can enable the persistence of bacteria such as *Staphylococcus aureus* within the body that lead to device failure and chronic disease.[160]

Biofilms are formed through a cycle with four stages. First, motile bacterial cells adhere to the material surface.[23,160] Bacterial cells can adhere reversibly, with non-specific forces or irreversibly with specific interactions with lectin or adhesin.[160] Next, adhered cells form a colony and secrete EPS. These bacterial colonies continue to grow and form into a mature biofilm, where cells can remain dormant until favorable conditions for infection arise. Dormancy, along with the colony structure, make biofilms characteristically resistant to antibiotics.[23,160,190] Finally, the biofilm disperses as aggregates or sessile bacterium to escape regions of accumulated bacterial waste and to start new regions of infection.[23]

Overall, implants with greater porosity have been implicated with a higher risk of biofilm formation (Figure 3C). This is especially true for small-scale porous materials that may be size exclusionary towards leukocytes but not bacteria (Figure 3C).[160] On titanium surfaces, Braem, et al. found greater bacterial adhesion to materials with pore sizes up to 150 μm or porosities greater than 15% because of greater surface roughness (Figure 3C).[155] Antibiotic prophylaxis can reduce the risk of infection, as well as using materials surface modified with nonadherent properties, anti-microbial agents, or specific topographies.[160,190,191] Feng, et al. also studied the effect of pore size on biofilm formation towards alumina materials with 0, 15, 25, 50, and 100 nm pore diameters *in vitro* and via computational modeling. Materials with either 15 or 25 nm pore sizes were found to reduce bacterial attachment through repulsive forces from the densely packed vertical pore sidewall within the anodic surfaces.[154] This effect of porosity on bacterial attachment is therefore also dependent on pore geometry and chemical composition of the material.

The correlation between porosity and infection is not as simple when studied in complex biological systems. The “race for the surface” describes the competition between host tissue and bacterial communities for space on the implant surface.[79,191] Tissue integration is therefore one of the most effective mitigation strategies for biofilm formation (Figure 3C).[79,160,191] Although porous mediums with large available surface areas can promote the adherence of biofilms, these porous materials also encourage tissue ingrowth, as described in section 3.1.5.

In an investigation of biofilm formation towards various dense and porous implants with 100 - 200 μm pores, Merritt, et al. found that porous materials were more susceptible to biofilm formation if the material became contaminated before or at the time of implantation. However, the porous materials were more resistant than dense materials if the infection occurred after 28 days, when the tissue had integrated into the material (Figure 3C).[156] Sclafani, et al. assessed biofilm formation towards high-density polyethylene (PHDPE, Medpor) materials with pores 100 - 250 μm and ePTFE with internodal pore sizes ranging from 10 - 30 μm. For both materials, implants became infected when inoculated with *S. aureus* immediately following surgery. When inoculated 14 days after implantation, PHDPE

materials with larger pores were found to be more resistant towards infection due to faster tissue integration. Other studies have shown tissue integration with ePTFE materials, so infection may not arise with these implants at later timepoints. Specific material composition may also confound the effect by pore size alone.[134] While porosity does increase the risk of biofilm formation, porous materials still provide benefits for tissue ingrowth which can decrease the risk of infection (Figure 3C). Therefore, surface treatments can be an effective strategy to control pathogen growth while still gaining the other advantages of biocompatibility that porous materials provide.

3.4. Calcification of porous materials

Biomaterial calcification or mineralization can commonly arise on devices contacting bone, blood, and urine and biofilms.[161] For orthopaedic implants, calicification results in osseointegration and therefore implant success.[192] For devices such as heart valves, calification can change the mechanical properties of the material, causing implant failure.[161] In general, mineralization occurs through electrostatic interactions between calcium and phosphate ions and an anionic material surface. For tissues or naturally derived scaffolds, this can occur at amino acids with anionic functional groups.[193] Osteoblasts mediate calcification in bone tissues.[192] In soft tissues, cytokines like TNF-α released by macrophages can cause osteogenic differenciation of local progenitor cells which enables mineral deposition.[161,193] Bacteria within a biofilm can release enzymes that lead to an increase in pH and promote hydroyapeptite crystal formation.[161] Calficication is not always cell mediated and can also form from free minerals in serum or urine.[158,161]

In the literature, it is wideley recognized that materials with higher porosity and pore size can initiate greater calcification (Figure 3D).[157–159,161] Comparing pHEMA hydrogels with varing porosities in buffer solutions, Lou, et al. found small deposits of calcium around implants with 58% porosity, large clumps of mineralization on implants with 96% porosity, and increased calcification around material defects.[159] In micro- and macroporous gels, Šprincl et al. found larger pores allowed for deeper calcification of subcuteanous implants (Figure 3D).[157] Also studied subcutaneously, Golomb, et al. found that greater calcium deposition towards porous films was an effect of the increased water capsity.[158] However, vascular graft implants with decreased porosity have been observed to initiate degenerative effects that initiated greater calcification. Wesolowski, et al. therefore concluded that materials with porosities greater than 5000 mL of water per minute per square centimeter of material at a pressure of 120 mmHg could prevent calcification and other responses.[132] Although it is true that porosity in general leads to greater calcium deposition, it is important to remember that inflammatory responses also initiate mechanisms of mineralization. Therefore, in complex biological systems, it is important to consider the local tissue response, and to prioritize material designs that reduce inflammatory responses.

4. Tissue-specific applications of porous biomaterials

As reiterated throughout this review, porosity can yield a more favorable host response, and many different methods exist to engineer biomaterials with precise porous architecture. Yet, medical devices are not always composed of porous materials. This is because various

tissues have unique functions and necessitate different aspects of biocompatibility, which impacts the design requirments for materials attempting to achieve local homeostasis. Further, tissues have unique microenvironments with different local immune cell populations that contribute to known variations in tissue specific host repsonses.[17–19,194] In this section, we review the impact of porous devices within specific tissue syestesm such as the subcutis, skeletal system, cardiovasuclar system, eye and nervous system, as well as the female reproductive tract. Table 4 summarizes these tissue-specific host reponses and functional impacts towards porous materials and Figure 4 shows some example surfaces relevent to the various tissues discussed. For details on tissue-specific biomaterial factors beyond porosity that are important for ECM-mimetic scaffolds, the reader is directed to an excellent review by Tonti, et al..[195]

4.1. Subcutaneous implants for material study and clinical uses in drug delivery

The subcutis exists as an adipocyte rich layer of tissue just beneath the skin surface, and primarily serves the body for thermal regulation, energy storage, and for protection from injuries.[219] Due to the presence of blood capillaries,[220] lymphatic plexus,[219] and the minimally invasiveness of accessing this compartment, the subcutis is widely used as a model to study the biomaterial FBR.[6,8–10,15,18,126,221] As detailed above (Section 3.1), porous materials with pore sizes approximately 40 μm in diameter show low fibrotic encapsulation, higher vascularization, and pro-healing responses from local immune cells, such as M2 polarized macrophages (Figure 3A).[7,9,10,80,126,222]

The vascularization and peripheral location of the subcutis makes this tissue compartment ideal for long-acting drug delivery implants for applications such as contraception, treatment of schizophrenia, management of opioid addiction, and HIV prevention.[220,223–227] Subcutaneously implanted porous devices have also shown greater fibrotic encapsulation than devices implanted in the intraperitoneal space or the epididymal fat pad in mice.[194] Although porous materials demonstrate improved biocompatibility over dense, non-textured surfaces,[15] some subcutaneous drug delivery systems are intentionally designed with low porosity to reduce drug release rates, as described in Section 2.3.[129,228] Sustained, long-acting drug release is critical for implantable drug delivery systems to improve patient adherence compared to a frequent daily dosing schedule, and fibrous capsule formation can impede drug release.[1,8,220,229] Implant re-insertion is also not practical in a timeframe of approximately less than six months.[224] Biocompatibility is also essential for enabling patient compliance towards these drug delivery systems, as patients will discontinue use of elective devices that cause discomfort.

Contraceptive implants – such as Nexplanon and its precursor Implanon, or Jadelle and its precursor Norplant – are the most widely used intradermal systems.[224,225] Nexplanon is a single cylindrical implant (2×40 mm) made of an ethylene vinyl acetate (EVA) polymer core loaded with the contraceptive agent etonogestrel and a drug-free EVA rate-controlling membrane, which has an effective duration of three years.[224,225,230,231] Jadelle is composed of 2 rods (2.5×43 mm each) that release the contraceptive levonorgestrel for up to five years within a polymer core and silicone rate-controlling membrane.[224,225] Information concerning the porosity and surface topography of these implants is limited.

However, similar hot-melt fabricated, drug-free EVA membranes exhibit microtextured but non-porous features.[232–234] Additionally, silicone implants have been described as smooth and solid, as opposed to porous.[235] Therefore, surface features of these implants lack microporous features which are associated with improved healing responses. Although adverse reactions have been reported,[236] such contraceptive implants have largely proven to be safe and tolerable.[237] In a study of tolerability of both levonorgestrel and etonogestrel subdermal implants, López del Cerro, et al. found one non-tolerable case of a FBR, out of 221 implants, which resulted in implant expulsion.[237] In another assessment of local side effects of Norplant by Alvarez, et al., 108 (35.6%) patients reported local hyperpigmentation of the skin, and 68 (22.4%) patients reported skin depression at the site of the implant due to a loss of subcutaneous tissue,[236] both which may be attributed to a FBR.[238]

A study of HIV preventative implants by Barrett, et al. indeed showed that dense implants created by hot-melt extrusion could achieve long-acting release of the investigational antiretroviral drug MK-8591 beyond 6 months. Interestingly, the implants became more porous over time, developing from the implant surface eroding into the core, with pores being created and increasing to ~2 μm wide with random geometry after full drug release. This possible porogen effect of drug particles within materials traditionally considered non-porous has been noted in other subcutaneous implant studies as well (Figure 4A).[239] The mechanism of drug release was therefore said to be mediated by solution permeation through voids evacuated by solubilized drug. The study does not include an assessment of the local tissue response.[129] In fact, another HIV implant study by Su, et al. describes overall lack of FBR assessment across other HIV implant studies, and reports an unacceptably adverse inflammatory reaction towards their tenofovir alafenamide fumarate loaded polyurethane membrane implant, despite lower inflammation observed against placebo implants.[240] Pharmaceuticals can contribute to adverse host responses, and therefore specific material and drug combinations must be assessed for their biocompatibility. Although porosity is not the sole arbiter of biocompatibility, material microarchitecture has shown to have a robust effect on resulting tissue outcomes and has been extensively studied in the subcutis. Therefore, porosity – and the balance of its effects on pharmacokinetics and biocompatibility – should be considered in the development of safe, long-acting devices.

4.2. Porosity for osseointegration in orthopedic and dental scaffolds

Bone interfacing implants such as prosthetic hips, knees, plates, pins or nails for fixation, bone cement, and oral implants represent some of the most common devices and biomaterials clinically implemented.[21,160] Such implants serve biomechanical functions, and therefore a mechanically stable, osseointegrative host response is needed for long-term biocompatibility.[192] The structure of bone tissue is either cortical (compact) or cancellous (spongy or trabecular, Figure 4B).[192,241] Compact bone comprises the hard outer surface of bone and is porous, yet dense with 3-12% porosity and pores 100-200 μm in diameter.[192,242] Osteons, or haversian systems, are the microscale structural unit of compact bone and are approximately 150-250 μm in diameter.[241,243] Cancellous tissue inside bone constitutes most of the bone tissue and has 50-90% porosity with irregularly patterned

trabeculae structures and bone marrow within the voids, which can measure up to 1 mm in diameter (Figure 4B).[241,242,244]

Bone tissue is continuously remodeling and is composed of blood vessels, cells, interstitial fluid, collagen fibers, and the mineral hydroxyapatite.[192,241,243] Bone building cells start as osteogenic stem cells, and differentiate into osteoblasts which synthesize the ECM components of bone, and range in diameter between 20-50 μm.[241,243] Osteoblasts mature into tissue maintaining osteocytes, and are embedded in bone lacuna measuring 15-20 μm in diameter, which have small radiating channels known as canaliculi filled with extracellular fluid and osteocyte processes for exchange of nutrients and wastes.[241,245] Conversely, osteoclasts enzymatically degrade bone for resorption as a means of continuing bone maintenance, and are derived from the fusion of many monocytes which results in a cell diameter ranging between 10-300 μm.[241,246] Thus, biomaterials that mimic the architecture of native bone and promote bone cell proliferation and integration could be ideal for biocompatible orthopedic devices (Figure 4C).

The primary pathway of bone regeneration and material osseointegration is similar to the traditional FBR (Section 3.1) but differs by cell specific responses. First, blood clotting occurs at the site of bone loss and the implant. In this first phase known as osteoconduction, the hematoma and specific activated platelets drive host reactions through the release of growth factors like TGF-β, IL-6, VEGF, fibroblast growth factor (FGF), and insulin growth factor (IGF) that recruit osteocytes and influence osteoblast action.[66,192,241,247] The callus then forms from collagen and cartilage to bridge fractured bone tissues and scaffolds. Through hormone signaling, the callus mineralizes requiring mainly calcium and phosphorous, but also magnesium, fluoride, and manganese.[241,243] Vitamins A, C, D, K, and B_{12} also contribute to osteoblast activity, bone protein synthesis, or calcium uptake.[241] The mineralized callus is then ideally remodeled into mature bone tissue.[192,241,247] Although bone tissue is mineralized, bone is also highly vascularized.[241] Therefore vascularization is essential for healthy scaffold-bone tissue integration.[248]

Due to the common use of orthopedic devices and the natively porous structure of bone, extensive research has been conducted with porous materials for osseointegration.[5,58,66,192,198–202,249–252] Unlike the subcutis, which has shown optimal host responses with approximately 40 μm pores (Figure 3A),[10,33,80] the critical pore size for bone tissue is suggested to be larger, yet a consensus on the specific size remains debated in the literature (Figure 3D). The necessity of porosity for osteogenesis has been well described in a review by Karageorgiou and Kaplan.[75] Various studies and reviews have defined 100 μm as the minimum required pore size for bone integration,[5,58,192,198–201] while other studies specify pores greater than 300 μm are optimal for bone growth.[196,197,203] However, other studies have stated that smaller pore sizes may be sufficient[5,66,202,249–251] Specifically, Hulbert, et al. found that pores greater than 100 μm promoted the greatest mineralized bone growth, and pores greater than 150 μm facilitated osteon formation within calcium aluminate implants placed midshaft of dog femurs.[199] However, Itälä, et al. claimed new bone ingrowth is independent of pore size within a range of 50-125 μm, which was assessed in titanium implants placed in non-load bearing regions of rabbit femurs. The authors also point out their observed response may be dependent on weight bearing conditions.[202]

Despite the known benefit of open pore structures, surgeons have been said to prefer the handling and stability of solid biomaterials.[242] Indeed, the addition of porosity can come at the sacrifice of mechanical stability, which is vital for orthopedic implants which often function for providing loadbearing support or mechanical fixation.[58,199] Clemow, et al. assessed porous coated titanium implants with pore sizes ranging between 175-350 μm and found percent bone ingrowth to be proportional to shear strength of the implant at the interface within the femoral medullary canal of dogs. Bone ingrowth was therefore also inversely proportional to the square root of pore diameter. This suggests that larger pore size is detrimental to bone ingrowth if the specific material choice has inadequate structural support, although all pore sizes assessed here were greater than 100 μm.[253] To mitigate the detrimental effects of porosity on material mechanics, modern approaches have focused on developing bone scaffolds with biomimetic architecture. One strategy to better mimic bone structure used polymer scaffolds with a porosity gradient, which captures both the mechanical integrity of dense cortical bone, and the higher porosity of cancellous bone, which enables tissue ingrowth.[58] Finite element modeling has also been used to elucidate how the specific design of pore microgeometry can effect parameters like mechanics, permeability, and surface area.[254] Future research into bone scaffold design therefore must consider material composition and microgeometry for stable osseointegration.

As is true for all implants, biofilm formation is also a concern for orthopedic implants.[20,160] Biofilm formation is an especially important consideration for dental scaffolds, considering the exposure to bacteria from the oral mucosa.[20,255] Osseointegration is important for dental implants as artificial teeth are often implanted into the jaw bone and anchored into place by healthy bone ingrowth.[247,255] Inflammation caused by dental implant biofilm, known as peri-implantitis, is known to contribute to bone tissue loss.[255] For these reasons, emerging research into bone integrative scaffolds show increased focus on biofilm prevention,[255] with strategies such as combined antibacterial nanoparticles[256] or probiotic biofilms, improving osseointegration.[257] In addition to material functionalization methods, it should be noted that implant osseointegration also reduces the available surface for biofilm infection, known as the “race for the surface” described in section 3.3.[79,191,255] Initial control over biofilm formation is needed to mitigate potential bone loss, which would better promote osseointegration, and in turn inhibit future infections. Future research is needed to further investigate effective prevention methods for biofilms, and to study the competing effect of large pore size on both biofilm formation and osseointegration.

4.3. Porous scaffolds for cardiovascular tissue integration

The cardiovascular system consists of the heart, the connecting blood vessels, and blood.[241] The heart and vessels are each composed of three tissue layers.[258] Blood contacts the heart endocardium or vessel tunica intima, which are continuous with each other, and are both composed of the endothelium and the basement membrane which these endothelial cells attach. Cardiac or smooth muscle cells compose the inner layers, known as the myocardium and tunica media in the heart and vessels, respectively. The external layers include the epicardium and the tunica adventitia which both consist of fibro-elastic connective tissue.[241,258] Biomaterial interactions between these tissue layers as well as blood (for blood tissue composition, see section 3.2) make cardiovascular devices a

unique challenge for biocompatibility. These complications include: thrombosis and device occlusion by clot (section 3.2); sepsis from biofilm formation (section 3.3); material calcification which deteriorates mechanical function (section 3.4); as well as fibrosis and stenosis caused by excessive tissue growth known as neointima hyperplasia.[150] Unlike bone tissue, where responses like calcification promote material biocompatibility, all these pathologies in the cardiovascular system can yield fatal responses. Porosity can increase tissue integration and decrease inflammatory responses (Figure 3A), but porosity can also promote platelet activation (Figure 3B) and calcification (Figure 3D). Here, we focus on biomaterials that are porous and intended for cardiovascular tissue integration.

The FBR occurs in cardiovascular tissue and has been studied especially in the heart. However, the resulting response also been observed to vary somewhat from what occurs in the subcutis. Luttikhuizen, et al. characterized a greater pro-inflammatory response towards supra-epicardially implanted collagen, as compared to subcutaneous implants. Further, greater MMP activity, especially MMP-9, was found within super-epicardial tissue, which resulted in greater degradation of these implants.[19] Despite this, the pore-size dependent FBR is comparable between cardiovascular and subcutaneous tissues. In a study by Madden, et al., sphere-templated, poly(2-hydroxyethyl methacrylate-co-methacrylic acid) (pHEMA-co-MAA) scaffolds with pore diameters 30-40 μm resulted in lower fibrous encapsulation and greater neovascularization, as opposed to non-porous, 20, 60, or 80 μm porous materials.[50] This response is similar to what was observed subcutaneously towards 34 μm pore diameter pHEMA implants by Sussman, et al. (see Sections 3.1.3 and 3.1.5).[10] Porous materials with controlled pore size therefore show positive implications when in contact with the cardiovascular tissue microenvironment, although hemocompatibility is not specifically addressed in these studies.

Appropriate cell integration within scaffolds also has implications for hemocompatibility. At the interface of blood and tissue, ECs act as an inert barrier against protein adhesion, platelet activation and consequently thrombosis.[181,205] ECs also change morphology in response to shear forces by elongating and aligning in the direction of blood flow. Cell alignment inhibits inflammatory responses in regions under high laminar shear by altering the interactions of flow forces on the ECM.[259] Creating biomaterial surfaces that can support endothelial cell growth is therefore an effective strategy for promoting hemocompatibility. As described in section 3.1.5, porosity contributes to microvascular EC migration and proliferation during angiogenesis. Studies of macrovascular endothelium growth *in vitro* generally show that lower porosity and smaller pore size materials facilitate greater EC attachment.[187,260–262] ECs are 10 to 40 μm in diameter and their growth is adherent-dependent. Proliferation is therefore limited on materials with pores that exceed cell size, specifically greater than 30 μm in diameter.[262,263] It should be noted that these monoculture models fail to capture the proliferative effect that local cell types like fibroblasts and the intimal ECM has on ECs. Pre-seeding porous scaffolds with fibroblasts has shown improved endothelialization and increased expression of growth factors like FGF, which is otherwise supplemented in EC growth media.[261,262,264–267] Therefore the effect of porosity on endothelialization should be considered using *in vivo* models, where the combined effect from the improved capacity for tissue infiltration can also be assessed.

While porosity is implicated in greater tissue integrative responses, neointima hyperplasia is known as an unfavorable response in the cardiovascular system.[206] In cardiovascular devices like stents, which open or support blood vessels in cases of coronary artery disease or aneurysm, stenosis by neointima hyperplasia is one of the main challenges for biocompatibility.[268,269] Stenosis can also occur at graft anastomosis.[270] Stents are often composed of porous metal meshes, and lower stent porosity is implicated with greater neointimal growth and less flexibility for device placement.[269] Wesolowski, et al. described the effect of porosity for vascular grafts, finding that increased porosity rather than material composition, had the greatest impact in reducing graft stenosis, which lead to tissue calcification in pigs, dogs, and even human.[132] Thrombosis may also arise from stenosis to altered hemodynamics and flow stasis.[271] Therefore, tissue ingrowth should be controlled not only to prevent occlusion, but also secondary responses such as thrombosis and calcification. The mechanism for neointimal hyperplasia is thought to arise in part by inflammatory mechanisms including pro-inflammatory cytokine signaling from macrophages.[270] Further, a dysfunctional or disrupted endothelium may enable neointimal growth.[268,270] Drug eluting stents used clinically effectively curb stenosis, and rely on agents which inhibit smooth muscle cell growth.[268] However, further improvements on cardiovascular host responses, including reduced stenosis, will require an environment which supports healthy EC growth.[268]

The effect of porosity on thrombus formation, endothelial cell growth, and neointimal hyperplasia *in vivo* has been extensively studied with ePTFE vascular constructs, as ePTFE grafts greater than 6 mm in diameter have shown great clinical outcomes.[205,207,272] For ePTFE, pore size is commonly reported as the internodal distance, as the microarchitecture is uniquely composed of nodes of material interconnected by thin polymer fibrils (Figure 4D).[142,205–207] Internodal distance and pore size is therefore also the same as fibril length.[206] Synthetic, small diameter vascular grafts with inner diameters less than 4 mm historically perform poorly in humans, with thrombus generation on the luminal graft surface being the most common causes of failure.[152,272] Biocompatible, small-diameter vascular grafts therefore remain an unmet clinical need, and a complex challenge for controlling host responses.

The unique surface topology of ePTFE has shown important impacts on cellular responses. However, the response to pore size in ePTFE grafts was also dependent on specific study methods and graft preparation. Campbell, et al. screened untreated ePTFE materials with internodal pore diameters ranging between 9 and 65 μm, and found increased pore size decreased the rate of patency of small diameter grafts tested in carotid or femoral arteries of dogs. Specifically, pores less than 22 μm resulted in greater rates of grafts with healthy tissue ingrowth, angiogenesis, and a thin neointima as opposed to grafts greater 34 μm.[206] Boyd, et al. found pre-seeding small diameter ePTFE grafts with ECs indeed increased the thrombus-free surface area as opposed to non-cellular ePTFE implanted in dog carotid arteries. Further, pre-clotted scaffolds with 40 μm internodal pore diameters had the greatest patency and largest thrombus-free surface with or without endothelial cell pre-treatments compared to grafts with either 28 or 52 μm pores.[205] Pore diameters are quantified prior to pre-clotting, so the resulting porosity of the treated scaffold is not reported. Porous, small diameter ePTFE grafts were also implanted in circulation and studied in baboons by Golden,

et al., which is the most relevant model for human hematology.[152,204,207] Here, implants were pre-clotted, and animals were treated with anticoagulants. Grafts with internodal pore sizes 60 and 90 μm enabled full integration of the endothelium across the graft length, while grafts with 10 or 30 μm pores failed to gain full luminal endothelium coverage. Interestingly, pore size also effected the mechanism of cellular ingrowth, as 10 and 30 μm porous grafts allowed for cell migration from the ends of the vessel whereas 60 and 90 μm porous grafts enabled transmural tissue ingrowth. However, at 3 months, 90 μm porous grafts also caused degradation of the intimal layer of the vessel and platelet accumulation, potentially caused by the lower mechanical integrity of the more porous material or by shearing effects.[207] While these studies highlight the various ways pore-size specificity of ePTFE can enable greater cardiovascular biocompatibility, the determined optimal pore sizes across these studies lack congruency.

In ePTFE and other vascular graft materials, porosity has been identified as a positive material feature which provides needed elasticity and potential tissue ingrowth to sustain long-term tissue stability. However, if porosity or pore size increases above some threshold, the increased tissue ingrowth leads to low patency, increased thrombosis, and poor biocompatibility. In a review of the effect of porosity on various vascular protheses, White proposes materials with 45 μm pore sizes may be optimal for maintaining viable tissue growth, avoiding fibrosis, and providing mechanical compliancy.[204] In a recent clinical trial, Drews, et al. studied autologous bone marrow-derived cells seeded onto large diameter vascular grafts made of fibrous poly(glycolic acid) and poly(caprolactone-co-lactide) (PCLA) with a comparable average pore diameter of 40 μm. Although grafts experienced high incidence of asymptomatic stenosis in humans within 6 months, simulations and ovine studies found this stenosis self-resolves and could be a part of the natural vessel healing process.[208] While this study further supports the use of 40 μm pores for supporting biocompatibility, this work also illustrates the need to better understand the pathology of biomaterial neovascularization in humans.

Other strategies have focused on designing grafts with materials other than ePTFE. One notable porous graft intended for hemodialysis is the sphere-templated silicone STARgraft developed by Healionics (Seattle, WA), which is currently being investigated in a clinical trial (NCT03916731).[44] Grafts with differing regions of porosity have also been recently investigated to mimic the layers of a native vessel. Wang, et al. developed a three-layered porous polyurethane graft using salt-leaching to mimic blood vessel anatomy.[273] Matsuzaki, et al. studied two layered grafts composed of a heparin PCLA co-polymer sponge surrounded by an electrospun PCL layer with pore sizes ranging from 4 to 15 μm.[89] In this study, larger pores did indeed allow for greater cell infiltration than 4 μm porous materials, but materials with pores greater than 4 μm also dilated under arterial blood pressure.[89] In both studies, poor mechanical matching resulted in the overall failure of both materials when studied in ovine models.[89,273] These studies illustrate that porosity is not the exclusive mediator of cardiovascular biocompatibility. Rather, mechanics of the graft – and the specific materials and fabrication methods that dictate these properties – are important design requirements. In another two-layered graft, de Valence, et al. assessed the effect of low and high porosity in either the luminal or external layers. Electrospun grafts with an approximate 11.3 μm pore size (81% porosity) in the luminal layer and 2 μm

pore size (62% porosity) in the external layer yielded the most favorable responses placed in the abdominal aortas of rats, with cellular ingrowth in the adventitia and without blood leakage (Figure 4E).[91] In addition to polymer selection and fabrication method, control over regional microgeometry may enable positive tissue integrative effects of porosity in cardiovascular materials, while mitigating the host responses including hemocompatibility and excessive tissue ingrowth.

4.4. Porous materials for neural and ophthalmic devices

Tissues of the brain and eye – specifically the anterior chamber and cornea – are immunologically unique from other tissues and are described to exist under a state of immune privilege.[274,275] The cells which compose these tissues have a limited capacity for regeneration. Therefore under this immune privileged state, inflammatory responses are dampened to prevent cell death.[274] Although brain and eye tissues are similar in this way, anatomical differences between the two tissues regulate this tolerogenic state through different mechanisms. For both tissues, this privileged state is maintained in part by the blood-brain barrier (BBB) or the blood-ocular barrier, which restricts the migration of inflammatory cells into these tissues.[276] The BBB also limits the passage of large proteins like cytokines and antibodies.[277]

Cells present within the eye and brain also dictate host responses in these unique tissue microenvironments. Like the subcutis, the eye cornea and sclera are rich in fibroblasts and collagen fibers. The cornea, however, is also lined with nonkeratinized stratified squamous epithelium on the outer surface and simple squamous epithelium at the interface of the anterior chamber.[241] Cell populations within the brain are especially unique. The primary functional cell type of the brain is the neuron, which responds to stimuli and transmits electrical signals across other neurons in the circuit.[241] Glial cells support neurons and include astrocytes and microglia, which are considered the main immune effector cells in the brain and are also the most relevant cell-types in the host response.[278] Similar to peripheral macrophages, microglia are phagocytes and secrete cytokines that will influence astrocyte responses.[241,277] Astrocytes are the most common glial cell sub-type and are known to have functions such as tissue support and maintenance of the BBB. In a process known as gliosis, astrocytes can also encapsulate foreign bodies or regions of tissue damage.[241,278,279] Gliosis is analogous to the traditional FBR, where microglia – along with macrophages – first adhere to the foreign material and signal for the activation of encapsulating astrocytes, a response which is comparable to fibroblasts in the fibrous capsule.[279] Indeed, biomaterial gliosis results in a thin surrounding layer of collagen and astrocyte feet known as the glial scar.[277,279] From an evolutionary standpoint, given the reduced capacity to fight foreign materials with inflammatory responses, “walling off” the material becomes the host’s best defense for protecting the surrounding tissue.

Immune cells like Tregs also influence the tolerogenic state of the eye, as these cells mount tolerogenic responses towards foreign antigens, as opposed to immunogenic.[275] In the anterior chamber of the eye, Tregs are also associated with the production and surface association of the anti-inflammatory cytokine TGF-β, both which enable immune suppression.[275,280] Tregs exist in small quantities in healthy brain tissues, but Treg

accumulation in brain tissues is also associated with protective responses against gliosis.[281] In the eye, anti-inflammatory soluble factors like cytokines are a necessary component of the immune tolerant state.[274,282] Cytokines like TGF-β, macrophage migration inhibitory factor (MIF), and IL-10 are found within the aqueous humor of the eye, and are known to suppress innate and adaptive immune responses like the complement system and natural killer (NK) cell cytolysis.[274,275,282–284] There still exists a need to better elucidate the role of these soluble, immunosuppressive factors in brain tissue.[274]

Although the eye and brain are described to be immune tolerant, biomaterial implants still undergo encapsulation either by fibrosis or glial scarring.[46,277–279,285,286] The reduced capacity to fight pathogens may also imply an increased risk of implant associated biofilm formation. Bacterial growth on intraocular lenses during cataract surgery can occur especially by the adhesion of bacteria from the conjunctival flora, thereby causing endophthalmitis.[213,214] Biofilms in the brain have been described to be a concern for neural probe signal impedance,[286] but otherwise there exists little research on this topic. Similarly, calcification towards biomaterials in the eye have been studied,[287] and although neural tissue calcification occurs under pathological states,[288] biomaterial calcification in the brain has not been described.

Various ophthalmic devices exist and are routinely used or implanted in patients, including but not limited to intraocular lenses (IOLs), contact lenses, glaucoma drainage devices, and orbital prostheses. Porous materials composing these devices have shown to provide greater mechanical flexibility, fluid flow, oxygen permeation, and cellular integration (Figure 4F).[46,48,212] Ophthalmic devices like IOLs do require a material structure with optical transparency. However, macroporous features are observed in some hydrogel contact lenses, and is thought to improve comfort by improving gas and water permeability to the cornea.[212] One promising application of porous materials in the eye is as a supracilliary drainage system to reduce intraocular pressure in uncontrolled glaucoma (Figure 4G). The iSTAR Medical (Wavre, Belgium) MINIject implant is made of flexible silicon with 27 μm sphere-templated pores. The flexible and porous structure of the MINIject has shown to conform to the shape of the eye, allow natural outflow rates of fluid through the pores, and reduces fibrosis. Glaucoma surgeries have a high risk of fibrosis, which causes device failure, and therefore must be mitigated.[45,46,48,289] In a recent clinical trial, the MINIject implant was found to effectively reduce intraocular pressure and reduce the need for medications across the two year study, without any serious adverse events.[46]

As described in Section 3, porosity can increase the risk of biofilm formation and calcification, which is also true for ophthalmic implants. Antibiotic loaded scleral bandages with 38 μm diameter pores have been proposed to mitigate both infection and fibrosis.[49] In an *in vitro* assessment of various orbital protheses, Toribio, et al. observed greater bacterial attachment on high density porous polyethylene implants with 100-500 μm pores, as compared to than non-porous silicone. However, the effects by material chemistry were not separately assessed from porosity, and despite any increased risk of infection, porous orbital implants are most commonly used.[214] Vijayasekaran, et al. also found samples of pHEMA sponges with pores on the order of 10 μm in diameter could calcify after 12-weeks implanted in a rabbit cornea model. Although this response was not compared to

smooth surfaces or pores with different sizes, this calcification was thought to arise by the penetration of physiologic fluids in the eye and growing tissue into the scaffold.[287] While porosity can be beneficial for ocular biocompatibility, devices in the eye can serve a wide variety of functions. The selection of smooth or porous topography therefore must consider the specific region, application, and risk.

For brain biocompatibility, gliosis has been presented as the main challenge.[277] Neural probes are the device with the most research and interest for brain biocompatibility, as the glial scar impedes the capacity to receive or transmit signals to neurons.[277–279,285,286] Long term access to the neural circuit is needed for brain computer interface applications, which hold the potential for restoring motor function in cases like paralysis or limb loss.[279] One factor which contributes to the magnitude of glial scarring is the mechanical mismatch between the probe material and brain tissue.[143,278,279,290] Porosity is one strategy which can improve material compliance.[48] Topography has also proven to impact gliosis, as nanoscale features have shown greater selectivity of neuronal coverage, rather than astrocytes, *in vitro*.[210,291] The increased surface area of textured and porous implants has even shown to reduce the electrical impedance of microelectrodes.[209,210] Bioactive, cell-seeded electrodes have also been promoted as a strategy for improving tissue responses.[292] Porous scaffolds can additionally permit such bioactivity, and has the potential to reduce fibrosis, as has been observed across other tissue microenvironments.[10,48,50] Indeed, lower glial encapsulation has been observed in early assessments of materials with pores 40 μm in diameter as compared to 100 μm or non-porous implants.[211] Porous materials therefore show great potential for improved host responses within brain tissue. More research is still needed to study such devices, as well as the mechanisms behind host responses in the brain.

4.5. Porous materials in the female reproductive tract

Like the eye and brain, both the male and female reproductive systems are immune privileged. For both these reproductive systems, this privileged state is necessary to prevent immune recognition of haploid germ cells as non-self.[274,293,294] The female reproductive tract (FRT) is especially interesting regarding the FBR, as tolerance towards paternal haploid cells, and embryos is required for fertility, and balanced tolerance towards the commensal vaginal microbiota is essential for general wellbeing and protection against disease.[294–296] Tregs are implicated as the primary mediator of this privileged state, especially during early pregnancy.[294,295] Ovarian steroids like estrogen and progesterone are known to regulate immune cell responses either directly or indirectly through cytokine signaling, and immune cell populations change temporally during the menstrual cycle.[294] Other factors such as MMPs are also known to change in response to the menstrual cycle and pregnancy, and contribute to the immune state of the FRT.[297,298]

The FRT is also interesting in the study of the FBR, as it is a common compartment for device placement – including tampons, diaphragms, and vaginal rings for drug delivery in the vaginal cavity, and contraceptive intrauterine devices (IUDs) in the uterus. Immune tolerance is observed towards medical implants like IUDs, which do not undergo fibrotic encapsulation, yet do induce inflammation as one mechanism of contraception.[299–302]

However, intrauterine fibrosis can arise, and is especially studied in cases of fallopian tubal occlusion. The occurrence of tubal occlusion has been observed to occur under acute stimuli such as material and mechanical stress from permanent contraceptive devices such as Essure,[303] large and repeated administration of chemical sclerosing agents,[304,305] or by chronic *chlamydia tachomatis* infection.[304,306] Considering that tissue integration is uncommon in the FRT and even detrimental to tissue function, as well as the bacteria tolerant nature of the FRT, biofilm formation is perhaps the most significant risk against material biocompatibility. Device biofilm formation can promote pathogen proliferation in the FRT, and potentially inhibit drug release for devices like contraceptive vaginal rings.[23] Thus, porous materials can cause negative health effects when resident in the FRT, and non-porous materials are commonly favorable for preventing the integration of bacteria into devices, especially IUDs and contraceptive rings (Figure 4H).[234]

Tampon use is a known risk factor for menstrual toxic-shock syndrome (mTSS).[215,216] Common use of extra-absorbent tampons starting in 1976 created a new niche for the common bacteria *Staphylococcus aureus* to interact with the human host environment, thereby contributing to the 1979-1980 epidemic of mTSS.[215,216] However, mTSS can arise without device use,[216] and reports of pessary use to treat uterine prolapse as early as the 19th century also describe possible cases of mTSS.[215] As a result of the porous structure which enables device absorbency, it is thought that a tampon with absorbed menses increases oxygen content within the typically anaerobic vaginal environment. This can allow for *S. aureus* growth, which releases TSS toxin 1 (TSST-1).[216,307] TSST-1 binds to vaginal epithelial cells, which induces chemokine signaling to macrophages and CD4+ T-cells. Consequently, these immune cells release a cytokine storm which manifests as mTSS – causing fever, hypotension, gastrointestinal effects, and/or alterations in consciousness.[216] However, incidence of mTSS with tampon use is rare. Efforts to reduce mTSS cases have included a standardization for labeling device absorbency, as well as recommendations for reduced wear time and use of the lowest needed absorbency rating.[216]

The IUD Dalkon shield is another interesting case of the possible detrimental effects of porosity in the FRT. The Dalkon shield was clinically available from 1971 until 1974 and varied from other IUDs in its shield-like shape of the device body. Most importantly, the Dalkon Shield also uniquely had a porous, multifilament removal string, or tail, which was needed as the larger body of the device required greater force to remove (Figure 4I).[217,218,308,309] Unlike other IUDs, which feature a monofilament removal string, the tail was found to wick bacterial species from the vaginal cavity into the uterus by capillary force.[217,218] Further, the small pore size between filaments excluded the passage of polymorphonuclear leukocytes through the IUD tail, so bacteria within the string remained protected against host immune responses.[218] In the United States, 11 deaths from generalized sepsis and 209 cases of septic spontaneous abortion were reported for women using the Dalkon shield, as well as a fivefold increase in pelvic inflammatory disorder cases as compared to other IUDs of the time.[217,309] Despite setbacks from this device, modern IUDs are safe and are the most effective contraceptive method available, with less than a 1% failure rate.[309]

Regardless of the history concerning porosity related health issues in the FRT, research on porous devices have been studied to address various FRT tissue disorders. Asherman syndrome is one uterine tissue disorder which causes abnormal endometrial tissue growth which causes the lining of the uterus to adhere. One strategy to mitigate this tissue growth is the placement of a biomaterial barrier within the uterus, such as an IUD.[310–312] To improve local coverage, a compressible porous scaffold was developed by Cai, et al. and studied in an intrauterine adhesion rat model. Scaffolds enabled the delivery of basic fibroblast growth factor (bFGF), which together led to statistically equivalent endometrium and gland growth as undamaged uterine tissue, and greater neovascularization. However, the porous scaffold alone initiated low endothelium and gland growth, and higher fibrosis – all comparable to the intrauterine adhesion group.[311] The added growth factor therefore appears to be the main contributor to healthy endometrial regeneration, rather than the porous scaffold.

Surgical mesh is another example of porous material commonly used to provide tissue reinforcement. In the case of pelvic organ prolapse, where pelvic organs herniate into the vagina, reinforcement with transvaginal mesh was previously a solution. However, due to mesh erosion and material exposure from chronic inflammation and poor tissue integration, the use of transvaginal mesh – but not intra-abdominal mesh – is now banned countries like the United States, United Kingdom, and Australia.[22,313] Mukherjee, et al. proposes the use of ECM-mimicking electrospun meshes seeded with endometrial mesenchymal stem cells (eMSCs) to improve vaginal tissue integration. Although electrospun meshes with eMSCs promisingly increase gene expression associated with angiogenesis, cell adhesion, and ECM regulation, these implant studies were conducted subcutaneously due to limitations of mouse FRT size.[313] Therefore, these results are not truly indicative of the FRT response. Accurate models of the human FRT are limited, but the specific microenvironment is necessary to capture this nonstandard host response which has been frequently misunderstood in the past.

5. Conclusion

Porous biomaterials are often designed to add functionality like increased perfusion, capillary uptake, mechanical compliance, agent release, and cellular infiltration. The capacity for three-dimensional cellular interactions within the material is perhaps the most notable, as these interactions have shown to improve biocompatibility by reducing the FBR. For these reasons, porosity has been identified as an important feature for improving host responses in clinically approved biomaterials such as surgical meshes[79] and Gore-Tex vascular grafts.[272] Porosity is also a key feature in many next-generation devices currently undergoing clinical trials, including sphere-templated devices such as STARgraft (Healionics, ClinicalTrials.gov identifiers: NCT03916731 and NCT04783779) for hemodialysis[44] and MINIject (iSTAR Medical, ClinicalTrials.gov identifiers including: NCT03374553, NCT03996200, NCT03624361), which is a glaucoma drainage device.[45,46] Additionally, electrospun materials have undergone clinical trials, such as EktoTherix™ (Neotherix Limited, ClinicalTrials.gov identifier: NCT02409628), a scaffold for dermatologic wounds, and others.[92]

Considering it is the interactions between the cells and scaffolds which affect cellular responses, specific pore size, rather than percent porosity, is perhaps the most important

measurement to consider when predicting host reactions. Porosity and larger pore size have also shown to effect thrombogenicity, increase risk for early biofilm infection, and increase available area to mineralize – pathologies which all may contribute to device failure. Depending on specific tissue location, these host reactions are known to vary in magnitude, risk, and can constitute as either a detriment or benefit. Therefore, better understanding of tissue physiology and mechanisms behind host responses are needed for engineering the next generation of medical devices with high biocompatibility. Further, better models and assessment tools are needed to elucidate and standardize measurements of biocompatibility, especially for thromboembolism and physiologically unique tissue environments like the female reproductive tract. Following these advances in the field, the design of scaffolds – including precision pore microgeometry, and selection of polymers with specific mechanical, or diffusional/degradation properties – can become better informed to balance the risks and benefits of porosity in a specific tissue compartment.

Acknowledgements

This work was supported by NIH/NIAID grants R01AI145483 and R01AI150325 to KAW, and the Howard Hughes Medical Institute (HHMI) [Gilliam Fellowship for Advanced Study to JH and KAW].

Author Biographies

Jamie L. Hernandez graduated with a B.S. in Biomedical Engineering in 2016 at the University of Arizona. She earned her Ph.D. from the Bioengineering Department at the University of Washington. Her thesis work focused on electrospun materials for drug delivery as subcutaneous implants and in application to the female reproductive tract.

Kim A. Woodrow is an Associate Professor at the University of Washington in the Department of Bioengineering. She earned a B.A. in Biochemistry and Molecular Biology from Wells College, and a M.S. and Ph.D. in Chemical Engineering from Stanford University. Her research is focused on applications of engineered biomaterials in mucosal infections and mucosal immunity.

References

[1]. Crawford L, Wyatt M, Bryers J, Ratner B, Adv. Healthc. Mater 2021, 2002153, 1.
[2]. Green JJ, Elisseeff JH, Nature 2016, 540, 386. [PubMed: 27974772]
[3]. Haugen HJ, Bertoldi S, Characterization of Morphology — 3D and Porous Structure, 2017.

[4]. Fukano Y, Usui ML, Underwood RA, Isenhath S, Marshall AJ, Hauch KD, Ratner BD, Olerud JE, Fleckman P, J. Biomed. Mater. Res. A 2010, 94A, 1172.

[5]. Annabi N, Nichol JW, Ph D, Zhong X, Ji C, Tissue Eng. Part B 2010, 16, 371.

[6]. Sharkawy AA, Klitzman B, Truskey GA, Reichert WM, J. Biomed. Mater. Res 1996, 37, 401.

[7]. Galperin A, Long TJ, Ratner BD, Biomacromolecules 2010, 11, 2583. [PubMed: 20836521]

[8]. Sharkawy AA, Klitzman B, Truskey GA, Reichert WM, J. Biomed. Mater. Res 1997, 40, 586.

[9]. Hady TF, Hwang B, Waworuntu ADPRL, Mulligan M, Ratner B, Bryers JD, J Tissue Eng Regen Med 2020, 15, 24. [PubMed: 33217150]

[10]. Sussman EM, Halpin MC, Muster J, Moon RT, Ratner BD, Ann. Biomed. Eng 2014, 42, 1508. [PubMed: 24248559]

[11]. Brown BN, Ratner BD, Goodman SB, Amar S, Badylak SF, Biomaterials 2012, 33, 3792. [PubMed: 22386919]

[12]. Bryers JD, Giachelli CM, Ratner BD, Biotechnol. Bioeng 2012, 109, 1898. [PubMed: 22592568]

[13]. Klopfleisch R, Jung F, J. Biomed. Mater. Res. - Part A 2017, 105, 927.

[14]. Ratner BD, Regen. Biomater 2016, 3, 107. [PubMed: 27047676]

[15]. Karp RD, Johnson KH, Buoen LC, Ghobrial HKG, Brand I, Brand KG, Natl Cancer Inst 1973, 51, 1275.

[16]. Brauker JH, Carr-Brendel VE, Martinson LA, Crudele J, Johnston WD, Johnson RC, J. Biomed. Mater. Res 1995, 29, 1517. [PubMed: 8600142]

[17]. Reid B, Gibson M, Singh A, Taube J, Furlong C, Murcia M, Elisseeff J, Tissue Eng J. Regen. Med 2015, 9, 315.

[18]. Hernandez JL, Park J, Yao S, Blakney AK, V Nguyen H, Katz BH, Jensen JT, Woodrow KA, Biomaterials 2021, 273, 120806. [PubMed: 33905960]

[19]. Luttikhuizen DT, van Amerongen MJ, de Feijter PC, Petersen AH, Harmsen MC, van Luyn MJA, Biomaterials 2006, 27, 5763. [PubMed: 16934325]

[20]. Spriano S, Yamaguchi S, Baino F, Ferraris S, Acta Biomater. 2018, 79, 1. [PubMed: 30121373]

[21]. Albrektsson T, Dahlin C, Jemt T, Clin. Implant Dent. Relat. Res 2014, 16, 155. [PubMed: 24004092]

[22]. MacDonald S, Terlecki R, Costantini E, Badlani G, Eur. Urol. Focus 2016, 2, 260. [PubMed: 28723371]

[23]. Hardy L, Cerca N, Jespers V, Vaneechoutte M, Crucitti T, Res. Microbiol 2017, 168, 865. [PubMed: 28232119]

[24]. Weber M, Steinle H, Golombek S, Hann L, Schlensak C, Wendel HP, Avci-adali M, Front. Bioeng. Biotechnol 2018, 6, 1. [PubMed: 29404323]

[25]. Xu L, Bauer J, Siedlecki CA, Colloids Surf B Biointerfaces 2014, 124, 49. [PubMed: 25448722]

[26]. Braune S, Latour RA, Reinthaler M, Landmesser U, Lendlein A, Jung F, Adv. Healthc. Mater 2019, 8, 1.

[27]. Rouquerol J, Avnir D, Fairbridge CW, Everett DH, Haynes JH, Pernicone N, Ramsay JDF, Sing KSW, Unger KK, Recommendations for the Characterization of Porous Solids, 1994.

[28]. Mishra R, Militky J, Venkataraman M, Nanoporous Materials, 2018.

[29]. Sayed E, Haj-Ahmad R, Ruparelia K, Arshad MS, Chang M, Ahmad Z, AAPS PharmSciTech 2017, 18, 1507. [PubMed: 28247293]

[30]. Ngo TD, Kashani A, Imbalzano G, Nguyen KTQ, Hui D, Compos. Part B 2018, 143, 172.

[31]. Yan Q, Dong H, Su J, Han J, Song B, Wei Q, Shi Y, Engineering 2018, 4, 729.

[32]. He F, Li D, He J, Liu Y, Ahmad F, Liu Y-L, Deng X, Ye Y-J, Yin D-C, Mater. Sci. Eng. C 2018, 86, 18.

[33]. Tylek T, Blum C, Hrynevich A, Schlegelmilch K, Schilling T, Dalton PD, Groll J, Biofabrication 2020, 12, 025007. [PubMed: 31805543]

[34]. Li S, Deng B, Grinthal A, Schneider-yamamura A, Kang J, Martens RS, Zhang CT, Li J, Yu S, Bertoldi K, et al., Nature 2021, 592, 386. [PubMed: 33854248]

[35]. Saltzman WM, Langer R, Biophys. J 1989, 55, 163. [PubMed: 2467696]

[36]. Ribas RG, Schatkoski VM, do TL Montanheiro A, de Menezes BRC, Stegemann C, Leite DMG, Thim GP, Ceram. Int 2019, 45, 21051.

[37]. Cox SC, Jamshidi P, Eisenstein NM, Webber MA, Burton H, Moakes RJA, Addison O, Attallah M, Shepherd DET, Grover LM, ACS Biomater. Sci. Eng 2017, 3, 1616. [PubMed: 33429647]

[38]. Fukano Y, Knowles NG, Usui ML, Underwood RA, Hauch KD, Marshall AJ, Ratner BD, Giachelli C, Carter WG, Fleckman P, et al., Wound Rep Reg 2006, 14, 484.

[39]. Isenhath SN, Fukano Y, Usui ML, Underwood RA, Irvin CA, Marshall AJ, Hauch KD, Ratner BD, Fleckman P, Olerud JE, J. Biomed. Mater. Res. Part A 2007, 83, 915.

[40]. Galperin A, Long TJ, Garty S, Ratner BD, J. Biomed. Mater. Res. A 2012, 101A, 775.

[41]. Long TJ, Takeno M, Sprenger CC, Plymate SR, Ratner BD, Tissue Eng. Part C 2013, 19, 738.

[42]. Underwood RA, Usui ML, Zhao G, Hauch KD, Takeno MM, Ratner BD, Marshall AJ, Shi X, Olerud JE, Fleckman P, J Biomed Mater Res A 2011, 98, 499. [PubMed: 21681942]

[43]. Fleckman P, Usui M, Zhao G, Underwood R, Maginness M, Marshall A, Glaister C, Ratner B, Olerud J, J. Biomed. Mater. Res. A 2012, 100A, 1256.

[44]. DeVita MV, Khine SK, Shivarov H, Kidney Int. Reports 2020, 5, 769.

[45]. Denis P, Hirneiß C, Reddy KP, Kamarthy A, Calvo E, Hussain Z, Ahmed IIK, Ophthalmol. Glaucoma 2019, 2, 290. [PubMed: 32672670]

[46]. Denis P, Hirneiß C, Durr GM, Reddy KP, Kamarthy A, Calvo E, Hussain Z, Ahmed IK, Br J Ophthalmol 2020, 0, 1.

[47]. Stein A, Microporous Mesoporous Mater. 2001, 45, 227.

[48]. Teng W, Long TJ, Zhang Q, Yao K, Shen TT, Ratner BD, Biomaterials 2014, 35, 8916. [PubMed: 25085856]

[49]. Galperin A, Smith K, Geisler NS, Bryers JD, Ratner BD, ACS Biomater. Sci. Eng 2015, 1, 593. [PubMed: 33434975]

[50]. Madden LR, Mortisen DJ, Sussman EM, Dupras SK, Fugate JA, Cuy JL, Hauch KD, Laflamme MA, Murry CE, Ratner BD, PNAS 2010, 107, 15211. [PubMed: 20696917]

[51]. Kim HJ, Kim U, Vunjak-novakovic G, Min B, Kaplan DL, Biomaterials 2005, 26, 4442. [PubMed: 15701373]

[52]. Zeltinger J, Sherwood JK, Graham DA, Müeller R, Griffith LG, Tissue Eng. 2001, 7, 557. [PubMed: 11694190]

[53]. Chiu Y, Larson JC, Isom A, Brey EM, Tissue Eng. Part C 2010, 16, 905.

[54]. Bryant SJ, Cuy JL, Hauch KD, Ratner BD, Biomaterials 2007, 28, 2978. [PubMed: 17397918]

[55]. Bernards DA, Desai TA, R. Soc. Chem 2010, 6, 1621.

[56]. Li WL, Lu K, Walz JY, Int. Mater. Rev 2012, 57, 37.

[57]. Kang H, Tabata Y, Ikada Y, Biomaterials 1999, 20, 1339. [PubMed: 10403052]

[58]. Di Luca A, Longoni A, Criscenti G, Mota C, Van Blitterswijk C, Moroni L, Biofabrication 2016, 8, 045007. [PubMed: 27725338]

[59]. Stokols S, Tuszynski MH, Biomaterials 2004, 25, 5839. [PubMed: 15172496]

[60]. Ho M, Kuo P, Hsieh H, Hsien T, Hou L, Lai J-Y, Wang D-M, Biomaterials 2004, 25, 129. [PubMed: 14580916]

[61]. Ricciardi R, Errico GD, Auriemma F, Ducouret G, Tedeschi AM, De Rosa C, Laupretre F, Lafuma F, Macromolecules 2005, 38, 6629.

[62]. Hou J, Jiang J, Guo H, Guo X, Wang X, Shen Y, Li Q, RSC Adv. 2020, 10, 10055. [PubMed: 35498611]

[63]. Lee J, Tan B, Cooper AI, Macromolecules 2007, 40, 1955.

[64]. Keskar V, Marion NW, Mao JJ, Gemeinhart RA, Tissue Eng. Part A 2009, 15, 1695. [PubMed: 19119921]

[65]. Annabi N, Mithieux SM, Weiss AS, Dehghani F, Biomaterials 2009, 30, 1. [PubMed: 18842297]

[66]. Whang K, Elenz DR, Nam EK, Tsai DC, Thomas CH, Nuber GW, Glorieux FH, Travers R, Sprague SM, Healy KE, Tissue Eng. 1999, 5, 35. [PubMed: 10207188]

[67]. Han SK, Song M, Choi K, Choi SW, Macromol. Mater. Eng 2021, 306, 2100114.

[68]. Ott HC, Matthiesen TS, Goh SK, Black LD, Kren SM, Netoff TI, Taylor DA, Nat. Med 2008, 14, 213. [PubMed: 18193059]

[69]. Liao J, Joyce EM, Sacks MS, Biomaterials 2008, 29, 1065. [PubMed: 18096223]

[70]. Jafarkhani M, Salehi Z, Bagheri Z, Aayanifard Z, Rezvan A, Doosthosseini H, Shokrgozar MA, Can. J. Chem. Eng 2020, 98, 62.

[71]. Chen W, Xu Y, Li Y, Jia L, Mo X, Jiang G, Zhou G, Chem. Eng. J 2020, 382, 122986.

[72]. Rowland CR, Colucci LA, Guilak F, Biomaterials 2016, 91, 57. [PubMed: 26999455]

[73]. Baiguera S, Del C, Lucatelli E, Kuevda E, Boieri M, Mazzanti B, Bianco A, Macchiarini P, Biomaterials 2014, 35, 1205. [PubMed: 24215734]

[74]. Smoak MM, Han A, Watson E, Kishan A, Grande-allen KJ, Cosgriff-hernandez E, Mikos AG, Tissue Eng. Part C 2019, 25, 276.

[75]. Karageorgiou V, Kaplan D, Biomaterials 2005, 26, 5474. [PubMed: 15860204]

[76]. Kang HW, Lee SJ, Ko IK, Kengla C, Yoo JJ, Atala A, Nat. Biotechnol 2016, 34, 312. [PubMed: 26878319]

[77]. Stewart SA, Dom J, Mcilorum VJ, Mancuso E, Lamprou DA, Donnelly RF, Larrañeta E, Pharmaceutics 2020, 12, 1.

[78]. Jakus AE, Geisendorfer NR, Lewis PL, Shah RN, Acta Biomater. 2018, 72, 94. [PubMed: 29601901]

[79]. Jordan SW, Fligor JE, Janes LE, Dumanian GA, Plast. Reconstr. Surg 2017, 141, 103.

[80]. Garg K, Pullen NA, Oskeritzian CA, Ryan JJ, Bowlin GL, Biomaterials 2013, 34, 4439. [PubMed: 23515178]

[81]. Chou SF, Carson D, Woodrow KA, Control J. Release 2015, 220, 584.

[82]. Xue J, He M, Liu H, Niu Y, Crawford A, Coates PD, Chen D, Shi R, Zhang L, Biomaterials 2014, 35, 9395. [PubMed: 25134855]

[83]. Xue J, He M, Liang Y, Crawford A, Coates P, Chen D, Shi R, Zhang L, J. Mater. Chem. B 2014, 2, 6867. [PubMed: 32261883]

[84]. Zahedi P, Rezaeian I, Ranaei-Siadat SO, Jafari SH, Supaphol P, Polym. Adv. Technol 2010, 21, 77.

[85]. Pilehvar-Soltanahmadi Y, Akbarzadeh A, Moazzez-Lalaklo N, Zarghami N, Artif. Cells, Nanomedicine Biotechnol 2016, 44, 1350.

[86]. Ardila DC, Tamimi E, Doetschman T, Wagner WR, Vande Geest JP, Control J. Release 2019, 299, 44.

[87]. Furdella KJ, Higuchi S, Behrangzade A, Kim K, Wagner WR, Vande Geest JP, Acta Biomater 2021, 123, 298. [PubMed: 33482362]

[88]. Hasan A, Memic A, Annabi N, Hossain M, Paul A, Dokmeci MR, Dehghani F, Khademhosseini A, Acta Biomater. 2013, 1. [PubMed: 24090989]

[89]. Matsuzaki Y, Iwaki R, Reinhardt JW, Chang YC, Miyamoto S, Kelly J, Zbinden J, Blum K, Mirhaidari G, Ulziibayar A, et al., Acta Biomater. 2020, 115, 176. [PubMed: 32822820]

[90]. Zhu T, Gu H, Zhang H, Wang H, Xia H, Mo X, Wu J, Acta Biomater. 2020, 16, 1.

[91]. de Valence S, Tille JC, Giliberto JP, Mrowczynski W, Gurny R, Walpoth BH, Möller M, Acta Biomater. 2012, 8, 3914. [PubMed: 22771455]

[92]. Stoddard RJ, Steger AL, Blakney AK, Woodrow KA, Ther. Deliv 2016, 7, 387. [PubMed: 27250537]

[93]. Ball C, Woodrow KA, Antimicrob. Agents Chemother 2014, 58, 4855. [PubMed: 24913168]

[94]. Blakney AK, Ball C, Krogstad EA, Woodrow KA, Antiviral Res. 2013, 100, S9. [PubMed: 24188701]

[95]. Blakney AK, Jiang Y, Woodrow KA, Drug Deliv. Transl. Res 2017, 7, 796. [PubMed: 28497376]

[96]. Huang C, Soenen SJ, van Gulck E, Vanham G, Rejman J, Van Calenbergh S, Vervaet C, Coenye T, Verstraelen H, Temmerman M, et al., Biomaterials 2012, 33, 962. [PubMed: 22018388]

[97]. Krogstad EA, Ramanathan R, Nhan C, Kraft JC, Blakney AK, Cao S, Ho RJY, Woodrow KA, Biomaterials 2017, 144, 1. [PubMed: 28802690]

[98]. Laborde ND, Leslie J, Krogstad E, Morar N, Mutero P, Etima J, Woodrow K, Van Der Straten A, PLoS One 2018, 13, 1.

[99]. Krogstad EA, Woodrow KA, Int. J. Pharm 2014, 475, 282. [PubMed: 25169075]

[100]. Carson D, Jiang Y, Woodrow KA, Pharm. Res 2016, 33, 125. [PubMed: 26286184]

[101]. Sill TJ, von Recum HA, Biomaterials 2008, 29, 1989. [PubMed: 18281090]

[102]. Wang C, Cao H, Biomed Res. Int 2019, 1.

[103]. Vaquette C, Cooper-white JJ, Acta Biomater. 2011, 7, 2544. [PubMed: 21371575]

[104]. Rnjak-Kovacina J, Wise SG, Li Z, Maitz PKM, Young CJ, Wang Y, Weiss AS, Biomaterials 2011, 32, 6729. [PubMed: 21683438]

[105]. Leong MF, Rasheed MZ, Lim TC, Chian KS, J Biomed Mater Res 2008, 91A, 231.

[106]. Wright LD, Andric T, Freeman JW, Mater. Sci. Eng. C 2011, 31, 30.

[107]. Gorna K, Gogolewski S, J. Biomed. Mater. Res. Part A 2006, 79, 963.

[108]. Nezafati N, Faridi-Majidi R, Pazouki M, Hesaraki S, Polym. Int 2019, 68, 1420.

[109]. Castilho M, Feyen D, Flandes-Iparraguirre M, Hochleitner G, Groll J, Doevendans PAF, Vermonden T, Ito K, Sluijter JPG, Malda J, Adv. Healthc. Mater 2017, 6, 1.

[110]. Yuan XY, Zhang YY, Dong C, Sheng J, Polym. Int 2004, 53, 1704.

[111]. Lien S, Ko L, Huang T, Acta Biomater. 2009, 5, 670. [PubMed: 18951858]

[112]. Sarasam AR, Samli AI, Hess L, Ihnat MA, V Madihally S, Macromol Biosci 2007, 7, 1160. [PubMed: 17703475]

[113]. V Madihally S, Matthew HWT, Biomaterials 1999, 20, 1133. [PubMed: 10382829]

[114]. Buj-Corral I, Bagheri A, Petit-Rojo O, Materials (Basel). 2018, 11, 1.

[115]. Rnjak-Kovacina J, Weiss AS, Tissue Eng. Part B 2011, 17, 365.

[116]. Nam JIN, Ph D, Huang YAN, Ph D, Agarwal S, Ph D, Lannutti J, Ph D, Tissue Eng. 2007, 13, 2249. [PubMed: 17536926]

[117]. Zonderland J, Rezzola S, Wieringa P, Moroni L, Biomed Mater 2020, 15, 1.

[118]. Eichhorn SJ, Sampson WW, J R Soc Interface 2005, 2, 309. [PubMed: 16849188]

[119]. Yang F, Xu CY, Kotaki M, Wang S, Ramakrishna S, J Biomater Sci Polym. Edn 2004, 15, 1483.

[120]. Gunathilake TMSU, Ching YC, Ching KY, Chuah CH, Polymers (Basel). 2017, 9, 1.

[121]. Garg T, Goyal AK, Expert Opin. Drug Deliv 2014, 11, 767. [PubMed: 24669779]

[122]. Braunecker J, Baba M, Milroy GE, Cameron RE, Int. J. Pharm 2004, 282, 19. [PubMed: 15336379]

[123]. Kumari PVK, Sharmila M, Rao YS, J. Pharm. Res. Int 2020, 32, 153.

[124]. Oh DS, Joon Y, Hong M, Han M, Kim K, Ceram. Int 2014, 40, 9583.

[125]. von Recum AF, Shannon CE, Cannon CE, Long KJ, van Kooten TG, Meyle J, Tissue Eng. 1996, 2, 241. [PubMed: 19877956]

[126]. Bota PCS, Collie AMB, Puolakkainen P, Vernon RB, Sage EH, Ratner BD, Stayton PS, J. Biomed. Mater. Res. A 2010, 95A, 649.

[127]. Ozpinar EW, Frey AL, Cruse G, Freytes DO, Tissue Eng. Part B 2021, 00, 1.

[128]. Doloff JC, Veiseh O, De Mezerville R, Sforza M, Perry TA, Haupt J, Jamiel M, Chambers C, Nash A, Aghlara-fotovat S, et al., Nat. Biomed. Eng 2021, DOI 10.1038/s41551-021-00739-4.

[129]. Barrett SE, Teller RS, Forster SP, Li L, Mackey MA, Skomski D, Yang Z, Fillgrove KL, Doto GJ, Wood SL, et al., Antimicrob. Agents Chemother 2018, 62, 1.

[130]. Khorshidi S, Solouk A, Mirzadeh H, Mazinani S, Lagaron JM, Sharifi S, Ramakrishna S, Tissue Eng J. Regen. Med 2016, 10, 715.

[131]. Bezuidenhout D, Davies N, Zilla P, ASAIO J 2002, 48, 465. [PubMed: 12296563]

[132]. Wesolowski SA, Fries CC, Karlson KE, De Bakey M, Sawyer PN, Plast. Reconstr. Surg 1962, 29, 131.

[133]. Milleret V, Hefti T, Hall H, Vogel V, Eberli D, Acta Biomater. 2012, 8, 4349. [PubMed: 22842036]

[134]. Sclafani AP, Thomas JR, Cox AJ, Cooper MH, Arch Otolaryngol Head Neck Surg 1997, 123, 328. [PubMed: 9076241]

[135]. Gouda R, Baishya H, Qing Z, Dev J. Drugs 2017, 6, 1.
[136]. Siepmann J, Peppas NA, Int. J. Pharm 2011, 418, 6. [PubMed: 21458553]
[137]. Khanafer K, Vafai K, Heat Mass Transf. und Stoffuebertragung 2006, 42, 939.
[138]. Korsmeyer RW, Gurny R, Doelker E, Buri P, Peppas NA, Int. J. Pharm 1983, 15, 25.
[139]. Guan J, Fujimoto KL, Sacks MS, Wagner WR, Biomaterials 2005, 26, 3961. [PubMed: 15626443]
[140]. Agrawal CM, Mckinney JS, Lanctot D, Athanasiou KA, Biomaterials 2000, 21, 2443. [PubMed: 11055292]
[141]. Lu L, Peter SJ, Lyman MD, Lai H, Leite SM, Tamada JA, Vacanti JP, Langer R, Mikos AG, Biomaterials 2000, 21, 1595. [PubMed: 10885732]
[142]. Ward WK, Slobodzian EP, Tiekotter KL, Wood MD, Biomaterials 2002, 23, 4185. [PubMed: 12194521]
[143]. Gori M, Vadalà G, Giannitelli SM, Denaro V, Di Pino G, Front. Bioeng. Biotechnol 2021, 9, 1.
[144]. Orenstein SB, Saberski ER, Kreutzer DL, Novitsky YW, J. Surg. Res 2012, 176, 423. [PubMed: 22099590]
[145]. Haase T, Krost A, Sauter T, Kratz K, Peter J, Kamann S, Jung F, Lendlein A, Zohlnhöfer D, Rüder C, Tissue Eng J. Regen. Med 2017, 11, 1034.
[146]. Rosengren A, Bjursten LM, J. Biomed. Mater. Res. - Part A 2003, 67, 918.
[147]. Yin Y, He XT, Wang J, Wu RX, Xu XY, Hong YL, Tian BM, Chen FM, Appl. Mater. Today 2020, 18, 100466.
[148]. Saino E, Focarete ML, Gualandi C, Emanuele E, Cornaglia AI, Imbriani M, Visai L, Biomacromolecules 2011, 12, 1900. [PubMed: 21417396]
[149]. Lucke S, Walschus U, Hoene A, Schnabelrauch M, Nebe JB, Finke B, Schlosser M, J Biomed Mater Res Part A 2018, 106A, 2726.
[150]. Deng X, Guidoin R, Med. Biol. Eng. Comput 2000, 38, 219. [PubMed: 10829417]
[151]. Wu WT, Jamiolkowski MA, Wagner WR, Aubry N, Massoudi M, Antaki JF, Sci. Rep 2017, 7, 1. [PubMed: 28127051]
[152]. Ratner BD, Horbett TA, Wagner WR, in Biomater. Sci., Elsevier, 2020, pp. 879–898.
[153]. Zhao J, Farhatnia Y, Kalaskar DM, Zhang Y, Bulter PEM, Seifalian AM, Int. J. Biochem. Cell Biol 2015, 68, 176. [PubMed: 26279141]
[154]. Feng G, Cheng Y, Wang SY, Borca-Tasciuc DA, Worobo RW, Moraru CI, npj Biofilms Microbiomes 2015, 1, 15022. [PubMed: 28721236]
[155]. Braem A, Van Mellaert L, Mattheys T, Hofmans D, De Waelheyns E, Schrooten J, Vleugels J, Geris L, Ann J, J. Biomed. Mater. Res. A 2014, 102A, 215.
[156]. Merritt K, Shafer JW, Brown SA, J. Biomed. Mater. Res 1979, 13, 101. [PubMed: 429378]
[157]. Šprincl L, Kopeček J, Lím D, Calcif. Tissue Res 1973, 13, 63. [PubMed: 4750794]
[158]. Golomb G, J. Mater. Sci. Mater. Med 1992, 3, 272.
[159]. Lou X, Vijayasekaran S, Sugiharti R, Robertson T, Biomaterials 2005, 26, 5808. [PubMed: 15949546]
[160]. Arciola CR, Campoccia D, Montanaro L, Nat. Rev. Microbiol 2018, 16, 397. [PubMed: 29720707]
[161]. Mosier J, Nguyen N, Parker K, Simpson CL, in Biomater. - Phys. Chem, 2018, pp. 37–60.
[162]. Anderson JM, Rodriguez A, Chang DT, Semin. Immunol 2008, 20, 86. [PubMed: 18162407]
[163]. Lord MS, Foss M, Besenbacher F, Nano Today 2010, 5, 66.
[164]. Jansson E, Tengvall P, Colloids Surfaces B Biointerfaces 2004, 35, 45. [PubMed: 15261055]
[165]. Richert L, Variola F, Rosei F, Wuest JD, Nanci A, Surf. Sci 2010, 604, 1445.
[166]. Woo KM, Chen VJ, Ma PX, J Biomed Mater Res A 2003, 67, 531. [PubMed: 14566795]
[167]. van Tienen TG, Heijkants RGJC, Buma P, de Groot JH, Pennings AJ, Veth RPH, Biomaterials 2002, 23, 1731. [PubMed: 11950043]
[168]. Klopfleisch R, Acta Biomater. 2016, 43, 3. [PubMed: 27395828]
[169]. Adusei KM, Ngo TB, Sadtler K, Acta Biomater. 2021, DOI 10.1016/j.actbio.2021.04.023.

[170]. Rodriguez A, MacEwan SR, Meyerson H, Kirk JT, Anderson JM, J. Biomed. Mater. Res. - Part A 2009, 90, 106.

[171]. Bartneck M, Heffels K, Pan Y, Bovi M, Zwadlo-klarwasser G, Groll J, Biomaterials 2012, 33, 4136. [PubMed: 22417617]

[172]. Klinge U, Klosterhalfen B, Birkenhauer V, Junge K, Conze J, Schumpelick V, J. Surg. Res 2002, 103, 208. [PubMed: 11922736]

[173]. Conze J, Rosch R, Klinge U, Weiss C, Anurov M, Titkowa S, Oettinger A, Schumpelick V, Hernia 2004, 8, 365. [PubMed: 15309687]

[174]. Brodbeck WG, Shive MS, Colton E, Nakayama Y, Matsuda T, Anderson JM, J. Biomed. Mater. Res 2001, 55, 661. [PubMed: 11288096]

[175]. Ghanaati S, Barbeck M, Orth C, Willershausen I, Thimm BW, Hoffmann C, Rasic A, Sader RA, Unger RE, Peters F, et al., Acta Biomater. 2010, 6, 4476. [PubMed: 20624495]

[176]. Barbeck M, Motta A, Migliaresi C, Sader R, Kirkpatrick CJ, Ghanaati S, Biomed Mater Res Part A 2015, 104A, 413.

[177]. Saleh LS, Bryant SJ, Drug Discov. Today Dis. Model 2018, 24, 13.

[178]. Whitaker R, Hernaez-Estrada B, Hernandez RM, Santos-Vizcaino E, Spiller KL, Chem. Rev 2021, 121, 11305. [PubMed: 34415742]

[179]. Krombach F, Münzing S, Allmeling AM, Gerlach JT, Behr J, Dörger M, Environ. Health Perspect 1997, 105 Suppl, 1261. [PubMed: 9400735]

[180]. Invitrogen, Countess Cell Data Sheet NIH/3T3, n.d.

[181]. Kalathottukaren MT, Kizhakkedathu JN, Mechanisms of Blood Coagulation in Response to Biomaterials: Extrinsic Factors, Elsevier Ltd., 2018.

[182]. Ratner BD, Biomaterials 2007, 28, 5144. [PubMed: 17689608]

[183]. Guidoin RG, Gosselin C, Rouleau C, Haggis GH, Boulay J, Awad J, J. Thorac. Cardiovasc. Surg 1975, 70, 152. [PubMed: 125367]

[184]. Hoffman AS, in Biomater. Interfacial Phenom. Appl, 1982, pp. 3–8.

[185]. Gaertner F, Massberg S, Semin. Immunol 2016, 28, 561. [PubMed: 27866916]

[186]. Ferraz N, Carlsson J, Hong J, Ott MK, J. Mater. Sci. Mater. Med 2008, 19, 3115. [PubMed: 18414999]

[187]. Lamichhane S, Anderson JA, Remund T, Sun H, Larson MK, Kelly P, Mani G, J. Biomed. Mater. Res. - Part A 2016, 104, 2291.

[188]. Ahmed M, Ghanbari H, Cousins BG, Hamilton G, Seifalian AM, Acta Biomater. 2011, 7, 3857. [PubMed: 21763798]

[189]. Keller N, Bruchmann J, Sollich T, Richter C, Thelen R, Kotz F, Schwartz T, Helmer D, Rapp BE, ACS Appl. Mater. Interfaces 2019, 11, 4480. [PubMed: 30645094]

[190]. Donlan RM, Costerton JW, Clin. Microbiol. Rev 2002, 15, 167. [PubMed: 11932229]

[191]. Busscher HJ, Van Der Mei HC, Subbiahdoss G, Jutte PC, Van Den Dungen JJAM, Zaat SAJ, Schultz MJ, Grainger DW, Sci. Transl. Med 2012, 4, 153rv10.

[192]. Wu X, Walsh K, Hoff BL, Camci-Unal G, Bioengineering 2020, 7, 1.

[193]. Wang X, Zhai W, Wu C, Ma B, Zhang J, Zhang H, Zhu Z, Chang J, Acta Biomater. 2015, 16, 81. [PubMed: 25641644]

[194]. Wang X, Maxwell KG, Wang K, Bowers DT, Flanders JA, Liu W, Wang L, Liu Q, Liu C, Naji A, et al., Sci. Transl. Med 2021, 13, 1.

[195]. Tonti OR, Larson H, Lipp SN, Luetkemeyer CM, Makam M, Vargas D, Wilcox SM, Calve S, Acta Biomater. 2021, 2, 1.

[196]. Kuboki Y, Jin Q, Takita H, J. Bone Jt. Surg 2001, 83, S105.

[197]. Tsuruga E, Takita H, Itoh H, Wakisaka Y, Kuboki Y, J. Biochem 1997, 121, 317. [PubMed: 9089406]

[198]. Robinson B, Hollinger J, Szachowicz, Brekke J, Otolaryngol. Neck Surg 1995, 112, 707.

[199]. Klawitter Hulbert SF JJ, J. Biomed. Mater. Res. Symp 1971, 2, 161.

[200]. Hulbert SF, Young FA, Mathews RS, Klawitter JJ, Talbert CD, Stelling FH, J. Biomed. Mater. Res 1970, 4, 433. [PubMed: 5469185]

[201]. Schliephake H, Neukam FW, Klosa D, Int. J. Oral Maxillofac. Surg 1991, 20, 53. [PubMed: 1850445]

[202]. Itälä AI, Ylänen HO, Ekholm C, Karlsson KH, Aro HT, J. Biomed. Mater. Res 2001, 58, 679. [PubMed: 11745521]

[203]. Götz HE, Müller M, Emmel A, Holzwarth U, Erben RG, Stangl R, Biomaterials 2004, 25, 4057. [PubMed: 15046896]

[204]. White RA, Trans Am Soc Artif Intern Organs 1988, XXXIV, 95.

[205]. Boyd KL, Schmidt S, Pippert TR, Hite SA, Sharp WV, J. Biomed. Mater. Res 1988, 22, 163. [PubMed: 3283132]

[206]. Campbell CD, Goldfarb D, Roe R, Ann. Surg 1975, 182, 138. [PubMed: 1211990]

[207]. Golden MA, Hanson SR, Kirkman TR, Schneider PA, Clowes AW, J. Vasc. Surg 1990, 11, 838. [PubMed: 2359196]

[208]. Drews JD, Pepper VK, Best CA, Szafron JM, Cheatham JP, Yates AR, Hor KN, Zbinden JC, Chang YC, Mirhaidari GJM, et al., Sci. Transl. Med 2020, 12, 1.

[209]. Yang J, Martin DC, Sensors Actuators, A Phys. 2004, 113, 204.

[210]. Chapman CAR, Chen H, Stamou M, Biener J, Biener MM, Lein PJ, Seker E, ACS Appl. Mater. Interfaces 2015, 7, 7093. [PubMed: 25706691]

[211]. Dryg I, Crawford L, Perlmutter S, Bryers J, Ratner B, in Soc. Biomater, n.d.

[212]. López-Alemany A, Compañ V, Refojo MF, J. Biomed. Mater. Res 2002, 63, 319. [PubMed: 12115764]

[213]. Elder MJ, Stapleton F, Evans E, Dart JKG, Eye 1995, 9, 102. [PubMed: 7713236]

[214]. Toribio A, Martínez-Blanco H, Rodríguez-Aparicio L, Ferrero M, Marrodán T, Fernández-Natal I, Int. J. Ophthalmol 2018, 11, 1895. [PubMed: 30588419]

[215]. Leidy LE, Med. Anthropol. Q 1994, 8, 198.

[216]. Schlievert PM, Davis CC, Clin. Microbiol. Rev 2020, 33, e00032. [PubMed: 32461307]

[217]. Tatum HJ, Schmidt FH, Mccarty M, Leary WMO, JAMA 1975, 231, 711. [PubMed: 1172860]

[218]. Bank HL, Williamson HO, Fertil. Steril 1983, 40, 334. [PubMed: 6884535]

[219]. Segura S, Requena L, Dermatol Clin 2008, 26, 419. [PubMed: 18793973]

[220]. Iyer SS, Barr WH, Karnes HT, Biopharm. Drug Dispos 2006, 27, 157. [PubMed: 16416503]

[221]. Woodard LN, Grunlan MA, ACS Macro Lett. 2018, 7, 976. [PubMed: 30705783]

[222]. Ward WK, J. Diabetes Sci. Technol 2008, 2, 768. [PubMed: 19885259]

[223]. Chen W, Yung BC, Qian Z, Chen X, Adv. Drug Deliv. Rev 2018, 127, 20. [PubMed: 29391221]

[224]. Weld ED, Flexner C, Curr Opin HIV AIDS 2020, 15, 33. [PubMed: 31764198]

[225]. Kleiner LW, Wright JC, Wang Y, Control J. Release 2014, 181, 1.

[226]. Cohen J, Science (80-.) 2019, 365, 309.

[227]. Dammerman R, Kim S, Adera M, Schwarz A, Clin. Pharmacol. Drug Dev 2018, 7, 298. [PubMed: 29420868]

[228]. Siegel RA, Kost J, Lange R, Control J. Release 1989, 8, 223.

[229]. Wood RC, Lecluyse EL, Fix JA, Biomaterials 1995, 16, 957. [PubMed: 8562786]

[230]. Palomba S, Falbo A, Di Cello A, Materazzo C, Zullo F, Gynecol. Endocrinol 2012, 28, 710. [PubMed: 22339096]

[231]. Schneider C, Langer R, Loveday D, Hair D, Control J. Release 2017, 262, 284.

[232]. Almeida A, Possemiers S, Boone MN, De Beer T, Quinten T, Van Hoorebeke L, Remon JP, Vervaet C, Eur. J. Pharm. Biopharm 2011, 77, 297. [PubMed: 21168487]

[233]. Grandi G, Timò A, Sammarini M, Chiara Del Savio M, Facchinetti F, Eur. J. Contracept. Reprod. Heal. Care 2020, 25, 60.

[234]. Miller L, Macfarlane SA, Materi HL, Contraception 2005, 71, 65. [PubMed: 15639076]

[235]. Frodel JL, Lee S, Arch Otolaryngol Head Neck Surg 1998, 124, 1219. [PubMed: 9821923]

[236]. Alvarez F, Brache V, Faundes A, Jorge A, Sousa MH, Contraception 2003, 68, 111. [PubMed: 12954523]

[237]. López del Cerro E, Diana CS, Canadas AMC, Cañadas C, Mirasol EG, Santos FG, Gómez MT, De Merlo GG, López E, Diana CS, et al., J. Obstet. Gynaecol. (Lahore). 2018, 38, 979.

[238]. Ramdhan RC, Simonds E, Wilson C, Loukas M, Oskouian RJ, Tubbs RS, Cureus 2018, 10, 1.

[239]. Stewart SA, Domínguez-Robles J, Utomo E, Picco CJ, Corduas F, Mancuso E, Amir MN, Bahar MA, Sumarheni S, Donnelly RF, et al., Int. J. Pharm 2021, 607, DOI 10.1016/j.ijpharm.2021.121011.

[240]. Su JT, Simpson SM, Sung S, Tfaily EB, Veazey R, Marzinke M, Qiu J, Watrous D, Widanapathirana L, Pearson E, et al., Anitmicrobial Agents Chemother. 2020, 64, 1.

[241]. Tortora GJ, Derrickson B, Principles of Anatomy & Physiology, John Wiley & Sons, Inc, 2012.

[242]. Kasten P, Beyen I, Niemeyer P, Luginbühl R, Bohner M, Richter W, Acta Biomater. 2008, 4, 1904. [PubMed: 18571999]

[243]. Qiu ZY, Cui Y, Wang XM, Natural Bone Tissue and Its Biomimetic, Elsevier Ltd, 2019.

[244]. Boyde A, Jones SJ, Microsc. Res. Tech 1996, 33, 92. [PubMed: 8845522]

[245]. Dallas SL, Prideaux M, Bonewald LF, Endocr. Rev 2013, 34, 658. [PubMed: 23612223]

[246]. Tiedemann K, Le Nihouannen D, Fong JE, Hussein O, Barralet JE, Komarova SV, Front. Cell Dev. Biol 2017, 5, 1. [PubMed: 28184371]

[247]. Sarinnaphakorn L, Di Silvio L, Surface-Modified Titanium to Enhance Osseointegration in Dental Implants, Woodhead Publishing Limited, 2009.

[248]. Xiao X, Wang W, Liu D, Zhang H, Gao P, Geng L, Yuan Y, Lu J, Wang Z, Sci. Rep 2015, 5, 1.

[249]. Martens M, Ducheyne P, De Meester P, Mulier JC, Arch. Orthop. Trauma. Surg 1980, 97, 111. [PubMed: 7458596]

[250]. Bobyn JD, Pilliar RM, Cameron HU, Weatherly GC, Clin. Orthop. Relat. Res 1980, *NO.* 150, 263.

[251]. Camron HU, Pilliar RM, Macnab I, J. Biomed. Mater. Res 1976, 10, 295. [PubMed: 1254617]

[252]. Spector M, J. Arthroplasty 1987, 2, 163. [PubMed: 3302108]

[253]. Clemow AJT, Weinstein AM, Klawitter JJ, Koeneman J, Anderson J, J. Biomed. Mater. Res 1981, 15, 73. [PubMed: 7348706]

[254]. Lu Y, Cheng LL, Yang Z, Li J, Zhu H, PLoS One 2020, 15, 1.

[255]. Kligman S, Ren Z, Chung C-H, Perillo MA, Chang Y-C, Koo H, Zheng Z, Li C, J. Clin. Med 2021, 10, 1641. [PubMed: 33921531]

[256]. Paris JL, Lafuente-Gómez N, Cabañas MV, Román J, Peña J, Vallet-Regí M, Acta Biomater. 2019, 86, 441. [PubMed: 30654210]

[257]. Tan L, Fu J, Feng F, Liu X, Cui Z, Li B, Han Y, Zheng Y, Yeung KWK, Li Z, et al., Sci. Adv 2020, 6, 1.

[258]. Arackal A, Alsayouri K, in StatPearls [Internet], 2020.

[259]. Hahn C, Schwartz MA, Nat Rev Mol Cell Biol 2009, 10, 53. [PubMed: 19197332]

[260]. Gao C, Li A, Yi X, Shen J, J. Appl. Polym. Sci 2001, 81, 3523.

[261]. Keun Kwon I, Kidoaki S, Matsuda T, Biomaterials 2005, 26, 3929. [PubMed: 15626440]

[262]. Narayan D, Venkatraman SS, J. Biomed. Mater. Res. - Part A 2008, 87A, 710.

[263]. Salem AK, Stevens R, Pearson RG, Davies MC, Tendler SJB, Roberts CJ, Williams PM, Shakesheff KM, J. Biomed. Mater. Res 2002, 61, 212. [PubMed: 12007201]

[264]. Gulbins H, Goldemund A, Anderson I, Haas U, Uhlig A, Meiser B, Reichart B, J. Thorac. Cardiovasc. Surg 2003, 125, 592. [PubMed: 12658201]

[265]. Choi M, Sultana T, Park M, Lee BT, Mater. Sci. Eng. C 2021, 120, 111659.

[266]. Xu L, Huang Y, Wang D, Zhu S, Wang Z, Yang Y, Guo Y, J. Mater. Sci. Mater. Med 2019, 30, 1.

[267]. Gospodarowicz D, Moran J, Braun D, Birdwell C, Proc. Natl. Acad. Sci. U. S. A 1976, 73, 4120. [PubMed: 1069301]

[268]. Blindt R, Vogt F, Astafieva I, Fach C, Hristov M, Krott N, Seitz B, Kapurniotu A, Kwok C, Dewor M, et al., J. Am. Coll. Cardiol 2006, 47, 1786. [PubMed: 16682302]

[269]. Lieber BB, Stancampiano AP, Wakhloo AK, Ann. Biomed. Eng 1997, 25, 460. [PubMed: 9146801]

[270]. Lee T, Roy-Chaudhury P, Adv. Chronic Kidney Dis 2009, 16, 329. [PubMed: 19695501]

[271]. Tang AY-S, Chan H-N, Tsang AC-O, Leung GK-K, Leung K-M, Yu AC-H, Chow K-W, J. Biomed. Sci. Eng 2013, 06, 812.

[272]. Begovac PC, Thomson RC, Fisher JL, Hughson A, Gallgen A, Eur J Vasc Endovasc Surg 2003, 25, 432. [PubMed: 12713782]

[273]. Wang C, Li Z, Zhang L, Sun W, Zhou J, Med. Eng. Phys 2020, 85, 1. [PubMed: 33081956]

[274]. Niederkorn JY, Nat. Immunol 2006, 7, 354. [PubMed: 16550198]

[275]. Cobbold SP, Adams E, Graca L, Daley S, Yates S, Paterson A, Robertson NJ, Nolan KF, Fairchild PJ, Waldmann H, Immunol. Rev 2006, 213, 239. [PubMed: 16972908]

[276]. Pachter JS, De Vries HE, Fabry Z, J. Neuropathol. Exp. Neurol 2003, 62, 593. [PubMed: 12834104]

[277]. Fournier E, Passirani C, Montero-Menei CN, Benoit JP, Biomaterials 2003, 24, 3311. [PubMed: 12763459]

[278]. Polikov VS, Tresco PA, Reichert WM, Neurosci J. Methods 2005, 148, 1.

[279]. Jorfi M, Skousen JL, Weder C, Capadona JR, J. Neural Eng 2015, 12, 011001. [PubMed: 25460808]

[280]. Nakamura K, Kitani A, Strober W, J. Exp. Med 2001, 194, 629. [PubMed: 11535631]

[281]. Ito M, Komai K, Mise-Omata S, Iizuka-Koga M, Noguchi Y, Kondo T, Sakai R, Matsuo K, Nakayama T, Yoshie O, et al., Nature 2019, 565, 246. [PubMed: 30602786]

[282]. Taylor AW, Eye 2009, 23, 1885. [PubMed: 19136922]

[283]. Apte RS, Niederkorn JY, J. Immunol 1996, 156, 2667. [PubMed: 8609381]

[284]. Apte RS, Sinha D, Mayhew E, Wistow GJ, Niederkorn JY, J. Immunol 1998, 160, 5693. [PubMed: 9637476]

[285]. Lacour SP, Courtine G, Guck J, Nat. Rev. Mater 2016, 1, 1.

[286]. Rivnay J, Wang H, Fenno L, Deisseroth K, Malliaras GG, Sci. Adv 2017, 3, DOI 10.1126/sciadv.1601649.

[287]. Vijayasekaran S, Chirila TV, Robertson TA, Lou X, Fitton JH, Hicks CR, Constable IJ, J. Biomater. Sci. Polym. Ed 2000, 11, 599. [PubMed: 10981676]

[288]. Baba Y, Broderick DF, Uitti RJ, Hutton ML, Wszolek ZK, Mayo Clin. Proc 2005, 80, 641. [PubMed: 15887432]

[289]. Grierson I, Minckler D, Rippy MK, Marshall AJ, Collignon N, Bianco J, Detry B, Johnstone MA, BMC Biomed. Eng 2020, 1, 1.

[290]. Chen R, Canales A, Anikeeva P, Nat. Rev. Mater 2017, 2, 1.

[291]. Webster TJ, Waid MC, McKenzie JL, Price RL, Ejiofor JU, Nanotechnology 2004, 15, 48.

[292]. Adewole DO, Serruya MD, Wolf JA, Cullen DK, Front. Neurosci 2019, 13, 1. [PubMed: 30740042]

[293]. Fijak M, Meinhardt A, Immunol. Rev 2006, 213, 66. [PubMed: 16972897]

[294]. Lee SK, Kim CJ, Kim D, Kang J, Immune Netw. 2015, 15, 16. [PubMed: 25713505]

[295]. Clark GF, Schust DJ, Front. Immunol 2013, 4, 1. [PubMed: 23355837]

[296]. Rose WA, Mcgowin CL, Spagnuolo RA, Eaves-pyles TD, Popov VL, Pyles RB, PLoS One 2012, 7, 1.

[297]. Nothnick WB, Semin Reprod Med 2008, 26, 494. [PubMed: 18951331]

[298]. Curry TE Jr., Osteen KG, Endocr. Rev 2003, 24, 428. [PubMed: 12920150]

[299]. Gupta PK, Malkani PK, Bhasin K, Contraception 1971, 4, 375.

[300]. Chou CH, Chen SU, Shun CT, Tsao PN, Yang YS, Yang JH, Sci. Rep 2015, 5, 1.

[301]. Sheppard BL, Contraception 1987, 36, 1.

[302]. El Sahwi S, Moyer DL, Contraception 1970, 2, 1.

[303]. Thurmond AS, Nikolchev J, Khera A, Scanlan RM, Maubon AJ-M, Machan L, Ball A, J. Women's Imaging 2004, 6, 75.

[304]. Growe RG, Luster MI, Fail PA, Lippes J, J. Reprod. Immunol 2013, 97, 159. [PubMed: 23453701]

[305]. Jensen JT, Hanna C, Yao S, Bauer C, Morgan TK, Slayden OD, Contraception 2015, 92, 96. [PubMed: 26070857]

[306]. Patton DL, Cosgrove Sweeney YT, Kuo C-C, J. Infect. Dis 1994, 169, 680. [PubMed: 8158051]

[307]. Hill DR, Brunner ME, Schmitz DC, Davis CC, Flood JA, Schlievert PM, Wang-Weigand SZ, Osborn TW, J. Appl. Physiol 2005, 99, 1582. [PubMed: 15932958]

[308]. Sivin I, Contraception 1993, 48, 1. [PubMed: 8403900]

[309]. Britton LE, Alspaugh A, Greene MZ, McLemore MR, Am J Nurs 2020, 120, 1.

[310]. Pabuccu R, Onalan G, Kaya C, Selam B, Ceyhan T, Ornek T, Kuzudisli E, Fertil. Steril 2008, 90, 1973. [PubMed: 18774563]

[311]. Cai Y, Wu F, Yu Y, Liu Y, Shao C, Gu H, Li M, Zhao Y, Acta Biomater. 2019, 84, 222. [PubMed: 30476581]

[312]. Jahanbani Y, Davaran S, Ghahremani-Nasab M, Aghebati-Maleki L, Yousefi M, Life Sci. 2019, 240, 117066. [PubMed: 31738881]

[313]. Mukherjee S, Darzi S, Paul K, Cousins FL, Werkmeister JA, Gargett CE, Front. Pharmacol 2020, 11, 1. [PubMed: 32116689]

[314]. Tatum HJ, Schmidt FH, Phillips DM, Contraception 1974, 11, 465.

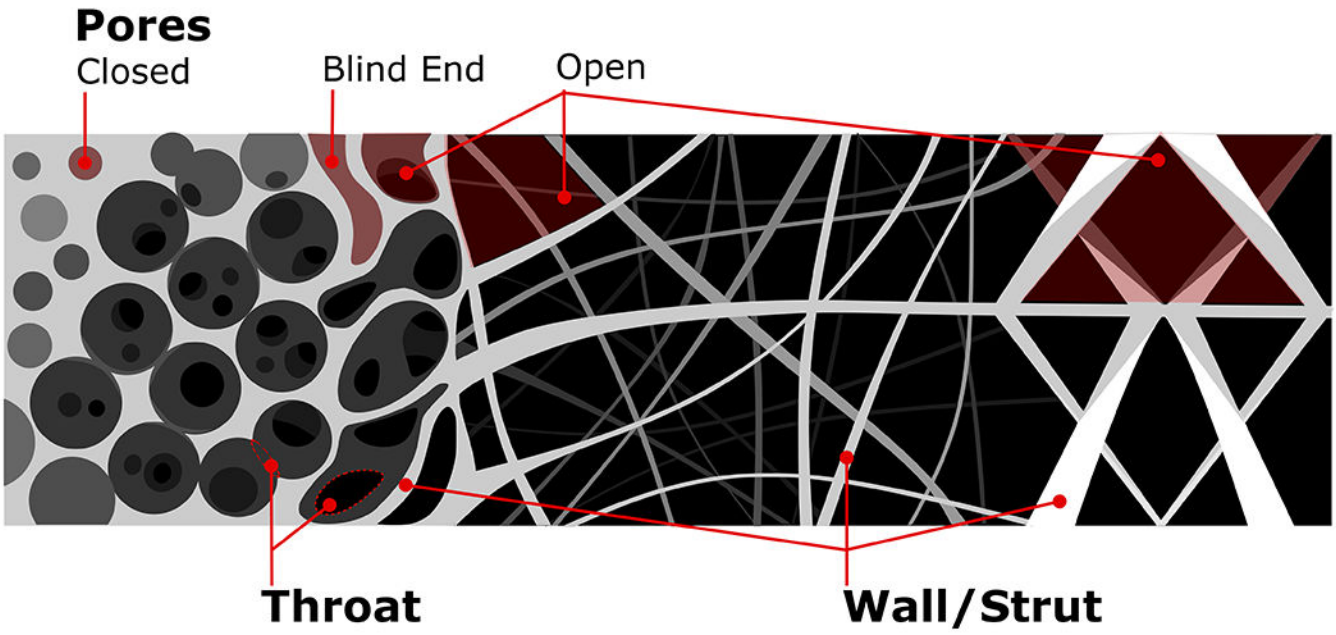

Figure 1.
Example architectures and relevant features of porous materials

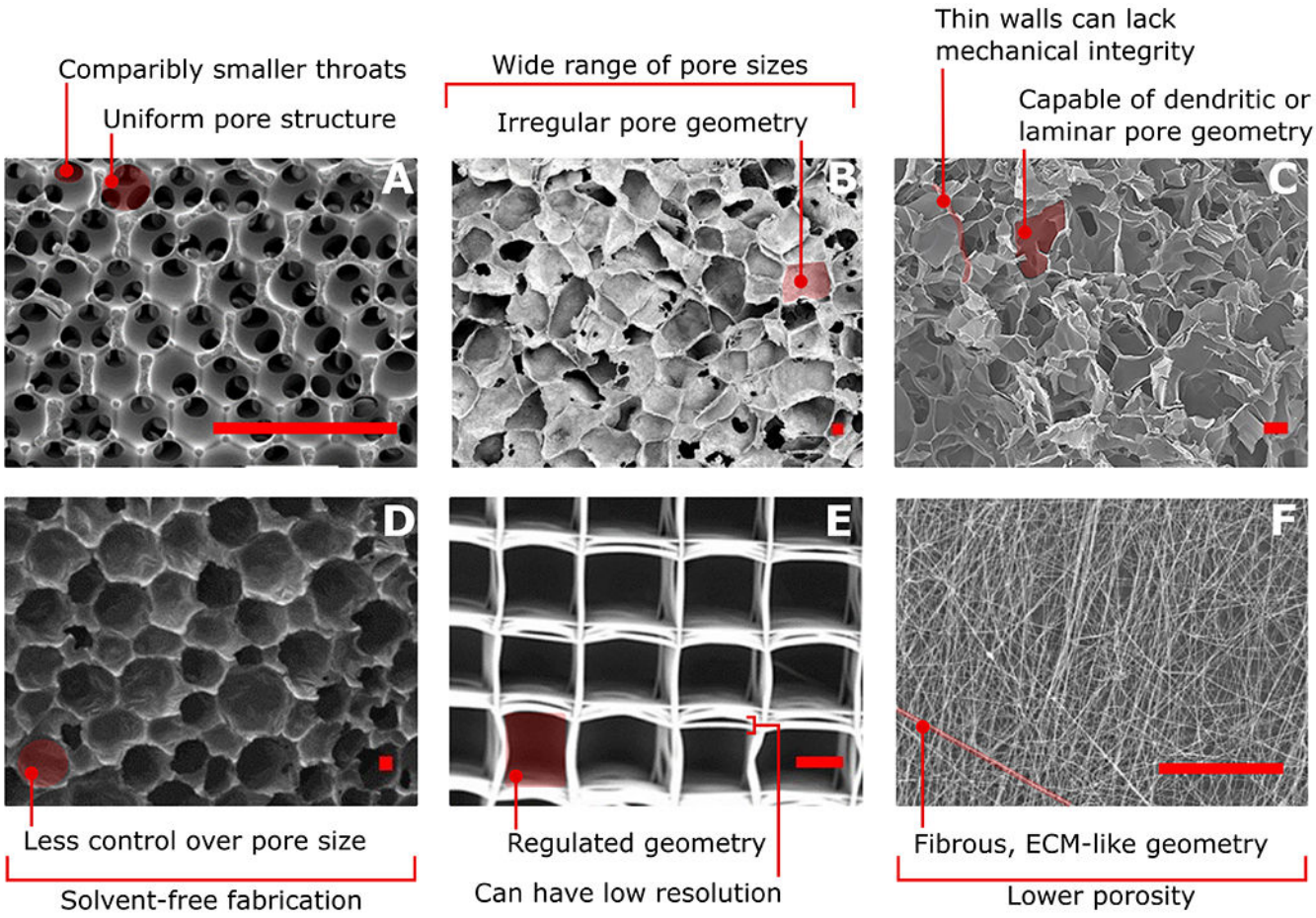

Figure 2.

SEM images of porous materials with example architectures and relevant features. Images include scaffolds created by: (A) sphere templating (reproduced with permission.[12] 2012, John Wiley and Sons); (B) salt-leaching (reproduced with permission.[107] 2006, John Wiley and Sons); (C) freeze-drying (reproduced with permission.[108] 2019, John Wiley and Sons); (D) gas-foaming (reproduced with permission.[67] 2021, John Wiley and Sons); (E) 3D-printed via melt electrospinning writing (reproduced with permission.[109] 2017, John Wiley and Sons); (F) conventional electrospinning (reproduced with permission.[110] 2004, John Wiley and Sons). Scale bars represent 100 μm.

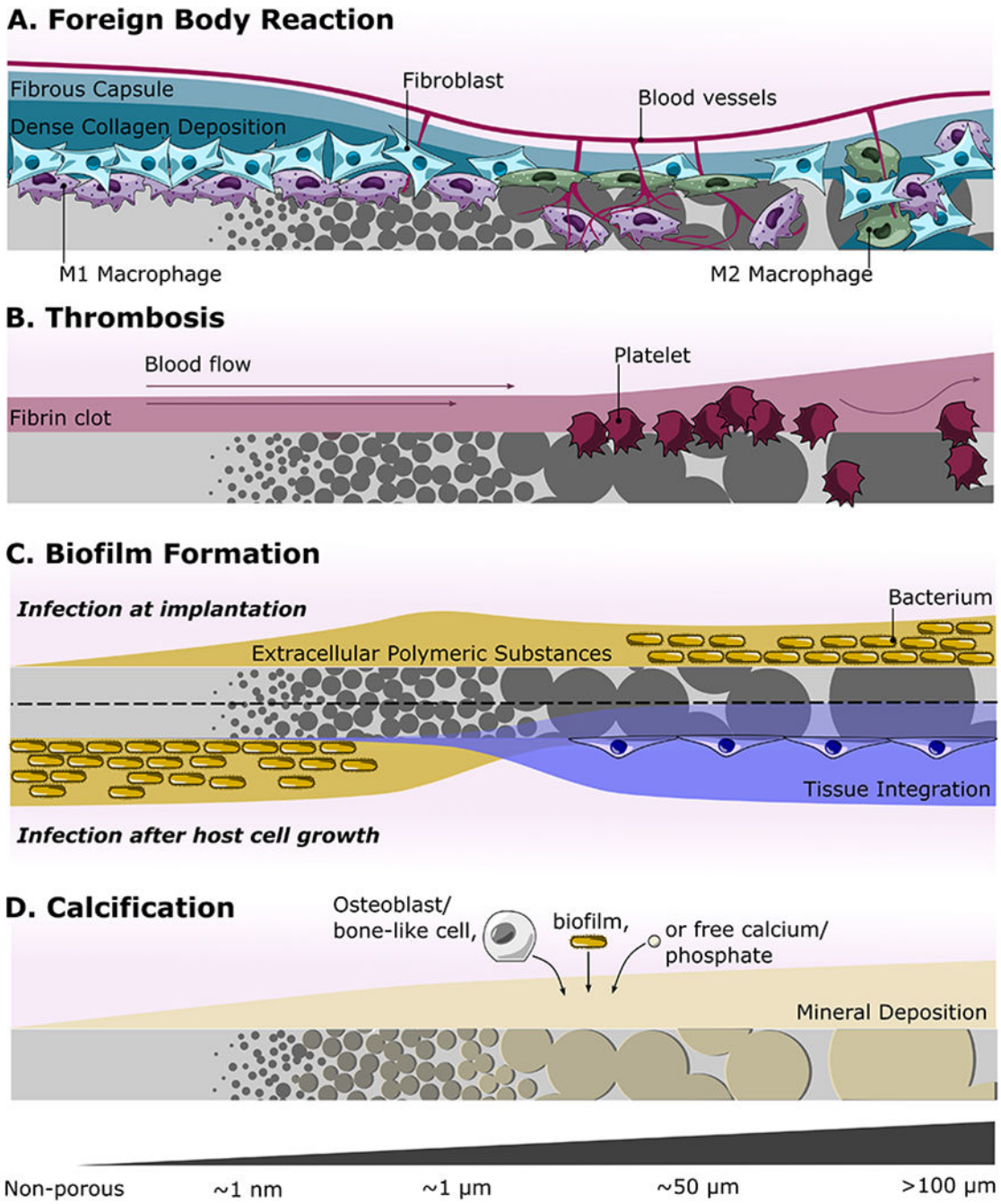

Figure 3.

Schematics summarizing biocompatibility trends reported in respect to biomaterial pore size. (A) In the FBR, non-porous materials induce thick fibrous capsule formation. Pores approximately 30-40 μm in diameter generate less of a capsule, greater angiogenesis, M1 macrophages within pores, and elongated M2 pores at the material surface. Larger pored materials generate mixed macropage populations and intrapore fibrosis.[10,12,33,80,146] (B) Thrombogenicity is associated with large porosity and surface roughness, especially with pores greater than 30 μm, and larger features which induce shear mediated platlet activation,

[133,150–153] (C) If infection occurs at time of implantation, greater biofilm formation occurs in materials with larger pores, but also in pores which are small enough to permit bacterium yet size exclusionary to immune cells. However, larger pores also allow for faster tissue integration which inhibits biofilm formation if infection occurs after host tissue growth. [134,155,156,160] (D) Greater calcification forms in more larger pored materials sourced from osteoblast-like cells, a biofilm, or free minerals.[157–159,161]

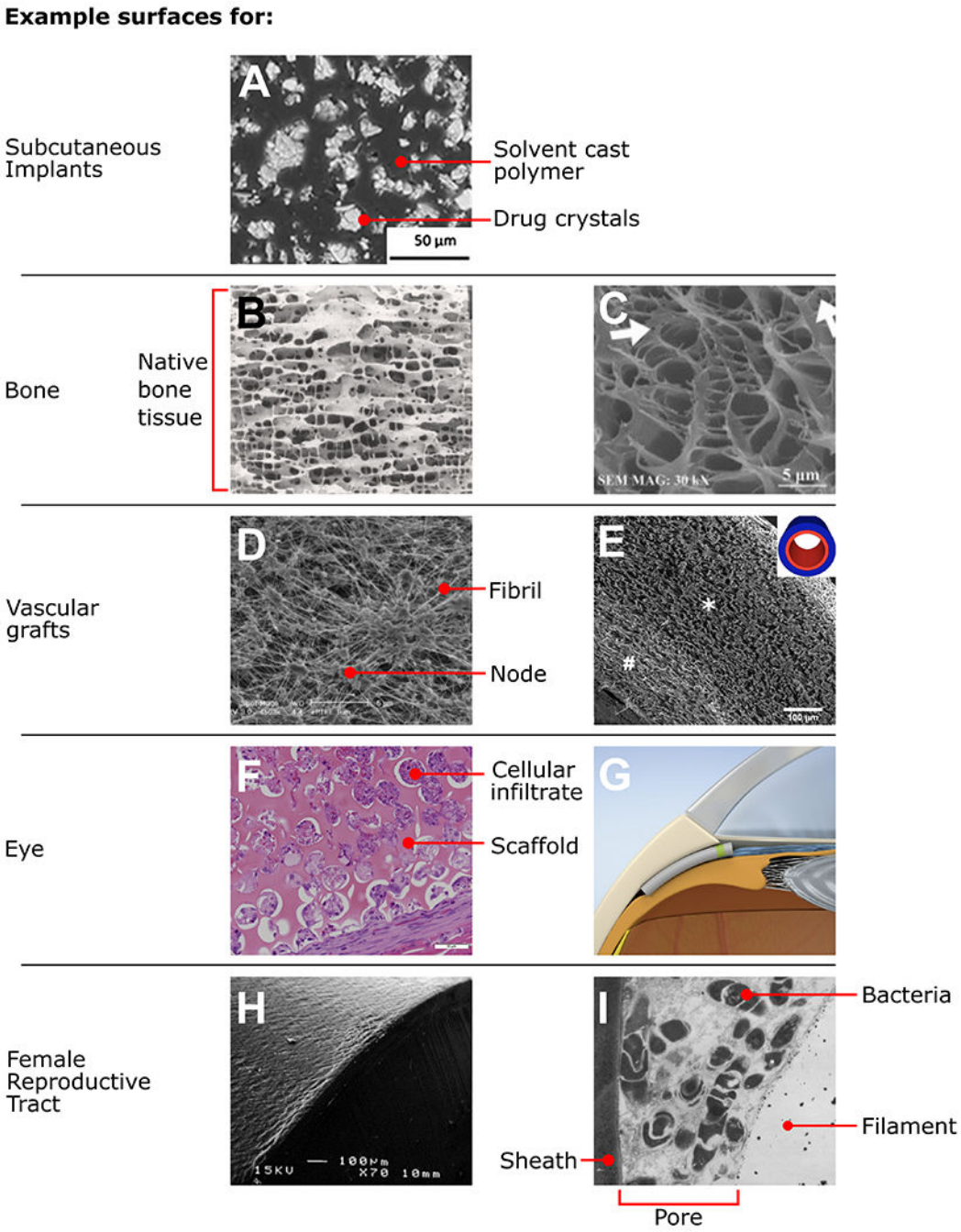

Figure 4.

Examples of surface topologies relevant to various tissue-specific applications. (A) Drug particulates act as porogens in an solvent cast subcutaneous implant (reproduced with permission.[239] 2021, Elsevier Inc.). SEM images show high porosity of (B) human cancellous bone tissue (reproduced with permission.[244] 1998,John Wiley and Sons) and (C) an example hybrid polymer scaffold which mimics native porosity, where arrows show regions with increased material wall porosity (reproduced with permission.[108] 2019, John Wiley and Sons). SEM images also show (D) the unique porous structure of ePTFE

(reproduced with permission.[142] 2002, Elsevier Inc.) and (E) hybrid vascular graft scaffolds with a low porosity luminal layer (#, red) and higher porosity adventitial layer (*, blue) (reproduced with permission.[142] 2002, Elsevier Inc.). Porosity in ophthalmic implants (F) enables cellular infiltration from surrounding ocular tissues (reproduced with permission.[48] 2014, Elsevier Inc.) and (G) has shown to reduce intraocular pressure in the MINIject glaucoma drainage device (iSTAR Medical SA) (reproduced with permission.[45] 2019, Elsevier Inc.). (H) Non-porous features are observed across the surface and cross-section of an EVA contraceptive vaginal ring (NuvaRing, Organon Pharmaceuticals) (reproduced with permission.[234] 2005, Elsevier Inc.). (I) The porous structure of the multifilament, Dalkon Shield tail allowed for bacterial infiltration (reproduced with permission.[314] 1974, Elsevier Inc.)

Table 1.

Porous biomaterial fabrication methods and the resulting porous features

Method	Range of pore diameters (μm)	Range of porosities (%)	Pore geometry	Method to ↑ pore size	Ref
Sphere templating	20 - 160	NA	Uniform, Spherical	↑ diameter of sacrificial beads	[9,10,42,47]
Salt leaching	15 - 970	30-92	Random	↑ salt particle size ↑ salt to polymer ratio	[51–53]
Freeze casting	1 - 500	~80	Laminar or dendritic	↑ ice crystal size, ↑ humidity; ↓ freezing rate, ↑ freezing/crosslinking temperature, omit excipients (i.e. glycerol, PVA) ↓ freeze/thaw cycles ↓ polymer concentration	[56,57,60,61,105,111–113]
Gas Foaming	100 - 600 (Conventional CO_2) 3.1 - 12.3 (CO_2/Water Emulsion)	67 - 88	Approximately spherical	↑ CO_2 fraction, ↑ pressure, hydrophilic polymer, biodegradable surfactant	[5,62–65]
3D Printing	40 - >300	41 – 65 67 - 94 (Salt leaching)	Pattern dependent	↑ filament spacing, Porogen leaching	[33,78,114]
Electrospinning	<5 - 140 (Conventional) 10 - 500 (Cryogenic) 105 - 192 (Mineral leaching)	48 – 54 (Conventional) 58 – 68 (Cryogenic) 78% (Salt leaching) 69 - 96 (Collected on perforated targets)	Random	↓ areal density; ↑ fiber diameter: ↑ polymer concentration, ↑ flow rate, ↓ voltage; Hybrid freezing method; Porogen leaching;	[80,103–105,115–119]

Table 2.

Summary of porosity effects on various features of biocompatibility

Response	Ideal pore size (μm or ↓/↑)	Ideal Porosity (Value or ↓/↑)	Model Tested	Ref
Reduction of fibrous capsule	30 - 40	↑	*in* vivo: C57BL/6 mouse percutaneous and subcutis, BAT-gal mouse subcutis, Sprague-Dawley rat abdominal wall	[4,9,10,144–146]
Macrophage polarization	M1: ≤20 or ≥60 (at surface), 34 (intrapore)	M1: ↓	*in vitro:* C57BL/6 mouse bone marrow-derived macrophages, human monocyte-derived macrophages	[9,10,12,33,80,147]
	M2: 30-50 (at surface), ≥360	M2: ↑	*in vivo*: BAT-gal mouse subcutis	
FBGC formation	<75	↓ for subcutaneous PU; ↑ for intramuscular PLA	*in vitro*: RAW 264.7 macrophages	[131,148,149]
			in vivo: BAT-gal mouse subcutis, male Wistar rat subcutis, male Lewis rat intramuscular	
Angiogenesis	≥5, ~40	↑	*in vivo*: BAT-gal mouse subcutis, C57BL/6 mouse subcutis, male Wistar rat subcutis, Lewis or Sprague-Dawley rat subcutis and abdominal wall	[1,5,10,12,16,131,145,146]
Hemocompatibility	<10 to limit platelet activation	↓ to limit platelet activation; <50 mL H_2O min^{-1} cm^2 at 120 mmHg to limit leakage with anti-coagulants	*in silico*: OpenFOAM computational fluid dynamic simulations	[132,133,150–153]
			in vitro: human blood (heparinized)	
			in vivo: pig, dog, human arterial grafts	
Biofilm Prevention	15-25 × 10^{-6} for anodic surface, ≥100 for infection 14d after implantation	↓ for infection at time of implantation; ↑ for infection after implantation	*in silico:* extended Derjaguin and Landau, Verwey and Overbeek model	[37,134,154–156]
			in vitro: E. coli O157:H7, E. coli K12, L. monocytogenes, S. aureus, S. epidermidis	
			in vivo: female outbred mouse subcutis with *S. aureus* injection, male Sprague-Dawley rat subcutis with *S. aureus* injection.	
Calcification	↑	↑; <5000 mL H_2O min^{-1} cm^2 at 120 mmHg to prevent inflammation	*in vitro*: $CaCl_2$ and K_2HPO_4 Tris buffer	[157–159]
			in vivo: Sabra male rat subcutis; Wistar rat and pig subcutis; pig, dog, human arterial grafts	

Adv Healthc Mater. Author manuscript; available in PMC 2023 May 01.

Table 3.

Macrophage phenotypes, inducers, and secretion signatures

Macrophage Phenotype	Inducers [a]	Elevated Expression/Secretion [a]	Ref
M1	LPS, IFN-γ, TNF-α, GM-CSF	TNF-α, IL-1β, IL-6, IL-12, IL-23, ROi	[1,12,168,177]
M2a	IL-4, IL-13	IL-10, TGF-β, IL-1ra	[1,12,168,177]
M2b	IC, TLR, LPS	IL-10, TNF-α, IL-1, IL-6, RNi, ROi	[1,12,168,177]
M2c	IL-10, TGF-β	IL-10, TGF-β, MMP9	[1,12,168,177]
M2d	IL-6, Adenosine	IL-10, IL-12, TNF-α, TGF-β, VEGF-A	[168,177]
FBGC	IL-4, IL-13, MMP9	ROS, MMP9, IL-1α, IL-6, IL-8, TNF-α, IL-10, TGF-β, MCP-1, TIMP-1, TIMP-2, VEGF	[13,162,168,175,176]

*a)*abbreviations: IL = interleukin, TNF = tumor necrosis factor, GM-CSF = granulocyte macrophage colony-stimulating factor, IFN = interferon, LPS = lipopolysaccaride, IC = immune complexes, TLR = toll like receptor, ROi = reactive oxygen intermediates, RNi = reactive nitrogen intermediates, ROS = reactive oxygen species, TGF = transforming growth factor, VEGF = vascular endothelial growth factor, MMP = matrix metalloproteinase, MCP = monocyte chemoattractant protein, TIMP = tissue inhibitor of metalloproteinases

Table 4.

Summary of tissue-specific impacts of porosity

Organ/Tissue	Local Host Response by Pore Size or Porosity	Functional Impacts of Increased Porosity	Ref
Skin/Subcutis	~40 μm minimizes FBR in mice and rats.	Increases rate of drug release.	[9,10,126,129]
Bone	≥100 μm, and specifically ≥300 μm, pores facilitate osseointegration subcutaneously in rats, and especially under load bearing conditions in dogs and rabbits.	Decreases mechanical stability.	[5,58,75,192,196–203]
Heart and blood vessels	30-40 μm reduces fibrosis, increases neovascularization in myocardial implants in rats. Porous effects for vascular grafts have variable conclusions.	High porosity can allow for hemorrhage with anticoagulated blood.	[50,132,204–208]
Brain	Increased porosity may increase mechanical compliance and topography, which reduces glial scarring in rats.	Increased surface area reduces impedance in neural probes.	[209–211]
Eye/Cornea and Anterior Chamber	27 μm pores do not undergo fibrosis in rabbits and humans.	Increases permeability towards water, gas, and fluids for drainage and improved comfort.	[45,46,48,212–214]
Female Reproductive Tract	Increased porosity increases risk of biofilm formation and infection in humans.	Facilitates absorption.	[215–218]